

A spectroscopic study of component C and the extended emission around I Zw 18

Yuri I. Izotov

Main Astronomical Observatory, Ukrainian National Academy of Sciences, Golosiiv, Kyiv 03680, Ukraine

izotov@mao.kiev.ua

Frederic H. Chaffee

W. M. Keck Observatory, 65-1120 Mamalahoa Hwy., Kamuela, HI 96743, USA

fchaffee@keck.hawaii.edu

Craig B. Foltz

MMT Observatory, University of Arizona, Tucson, AZ 85721, USA

cfoltz@as.arizona.edu

Trinh X. Thuan

Astronomy Department, University of Virginia, Charlottesville, VA 22903, USA

txt@virginia.edu

Richard F. Green

National Optical Astronomy Observatories, Tucson, AZ 85726, USA

rgreen@noao.edu

Polychronis Papaderos and Klaus J. Fricke

Universitäts-Sternwarte, Geismarlandstrasse 11, D-37083 Göttingen, Germany

papade@uni-sw.gwdg.de, kfricke@uni-sw.gwdg.de

and

Natalia G. Guseva

Main Astronomical Observatory, Ukrainian National Academy of Sciences, Golosiiv, Kyiv 03680, Ukraine

guseva@mao.kiev.ua

Received ; accepted

ABSTRACT

Long-slit Keck II¹, 4m Kitt Peak², and 4.5m MMT³ spectrophotometric data are used to investigate the stellar population and the evolutionary status of I Zw 18C, the faint C component of the nearby blue compact dwarf galaxy I Zw 18. Hydrogen H α and H β emission lines are detected in the spectra of I Zw 18C, implying that ionizing massive stars are present. High signal-to-noise Keck II spectra of different regions in I Zw 18C reveal H γ , H δ and higher order hydrogen lines in absorption. Several techniques are used to constrain the age of the stellar population in I Zw 18C. Ages derived from two different methods, one based on the equivalent widths of the H α , H β emission lines and the other on H γ , H δ absorption lines are consistent with a 15 Myr instantaneous burst model. We find that a small extinction in the range $A_V = 0.20 - 0.65$ mag is needed to fit the observed spectral energy distribution of I Zw 18C with that model. In the case of constant star formation, all observed properties are consistent with stars forming continuously between ~ 10 Myr and $\lesssim 100$ Myr ago. We use all available observational constraints for I Zw 18C, including those obtained from *Hubble Space Telescope* color-magnitude diagrams, to argue that the distance to I Zw 18 should be as high as ~ 15 Mpc. The deep spectra also reveal extended ionized gas emission around I Zw 18. H α emission is detected as far as $30''$ from it. To a B surface brightness limit of ~ 27 mag arcsec⁻² we find no observational evidence for extended stellar emission in the outermost regions, at distances $\gtrsim 15''$ from I Zw 18.

Subject headings: galaxies: evolution — galaxies: formation — galaxies: ISM — galaxies: starburst — galaxies: stellar content

1. Introduction

I Zw 18 remains the most metal-poor blue compact dwarf (BCD) galaxy known since its discovery by Sargent & Searle (1970). Later spectroscopic observations by Searle & Sargent (1972), Lequeux et al. (1979), French (1980), Kinman & Davidson (1981), Pagel et al. (1992), Skillman

¹W.M. Keck Observatory is operated as a scientific partnership among the California Institute of Technology, the University of California and the National Aeronautics and Space Administration. The Observatory was made possible by the generous financial support of the W.M. Keck Foundation.

²Kitt Peak National Observatory (KPNO) is operated by the Association of Universities for Research in Astronomy, Inc., under cooperative agreement with the National Science Foundation.

³The MMT is a joint facility of the Smithsonian Institution and the University of Arizona.

& Kennicutt (1993), Martin (1996), Izotov & Thuan (1998), Vílchez & Iglesias-Páramo (1998), Izotov & Thuan (1999) and Izotov et al. (1999) have confirmed its low metallicity with an oxygen abundance of only $\sim 1/50$ the solar value.

Zwicky (1966) described I Zw 18 as a double system of compact galaxies, which are in fact two bright knots of star formation with an angular separation of $5''.8$. These two star-forming regions (Fig. 1) are referred to as the brighter northwest (NW) and fainter southeast (SE) components. Later studies by Davidson, Kinman & Friedman (1989) and Dufour & Hester (1990) have revealed a more complex optical morphology with additional diffuse features. The most prominent diffuse feature, hereafter I Zw 18C (Fig. 1), is a blue irregular star-forming region $\sim 22''$ northwest of the NW component. Dufour, Esteban & Castañeda (1996a), Izotov & Thuan (1998) and van Zee et al. (1998) have shown I Zw 18C to have a systemic radial velocity equal to that of the ionized gas in the NW and SE components, thus establishing its physical association to I Zw 18. Furthermore, van Zee et al. (1998) have shown that I Zw 18C is embedded in a common H I envelope with the NW and SE components.

Many studies have been focused on the evolutionary state of I Zw 18. Searle & Sargent (1972) and Hunter & Thronson (1995) have suggested that it may be a young galaxy, recently undergoing its first burst of star formation. The latter authors concluded from *Hubble Space Telescope* (*HST*) images that the colors of the diffuse unresolved component surrounding the SE and NW regions are consistent with a population of B and early A stars, i.e. with no evidence for older stars. Ongoing massive star formation in I Zw 18 is implied by the discovery of a population of Wolf-Rayet stars in the NW component (Izotov et al. 1997a; Legrand et al. 1997).

From the analysis of color-magnitude diagram (CMD) based on *HST* images, Dufour et al. (1996b) concluded that star formation in I Zw 18 began at least 30 – 50 Myr ago and continuing to the present. Martin (1996) and Dufour et al. (1996b) have discussed the properties of expanding superbubbles of ionized gas driven by supernova explosions and have inferred dynamical ages of 15 – 27 Myr and 13 – 15 Myr respectively.

Recently, Aloisi, Tosi & Greggio (1999) have discussed the star formation history in I Zw 18 using the same *HST* WFPC2 archival data (i.e. those by Hunter & Thronson (1995) and Dufour et al. (1996b)). They compared observed CMDs and luminosity functions with synthetic ones and concluded that there were two episodes of star formation in I Zw 18, the first one occurring over the last 0.5 – 1 Gyr, an age more than 10 times larger than that derived by Dufour et al. (1996b), and the second one with more intense activity taking place between 15 and 20 Myr ago. No star formation has occurred within the last 15 Myr. Östlin (2000) from *HST* NICMOS *J* and *H* observations concluded that a 1 – 5 Gyr old stellar population is present.

The component I Zw 18C has not been studied in such detail mainly because of its faintness. Its flux-calibrated optical spectra (Izotov & Thuan 1998; van Zee et al. 1998) reveal a blue continuum with weak Balmer absorption features and faint H α and H β in emission. Such spectral features suggest that the H II region is probably ionized by a population of early B stars.

Dufour et al. (1996b) found in a $(B - V)$ vs. V CMD analysis of I Zw 18C a well-defined upper stellar main sequence indicating an age of the blue stars of ~ 40 Myr. However, numerous faint red stars were also present in the CMD, implying an age of $100 - 300$ Myr. Those authors concluded that I Zw 18C consists of an older stellar population with an age of several hundred Myr, but which has experienced recently a modest starburst in its southeastern half as evidenced by the presence of blue stars and $H\alpha$ emission. Aloisi et al. (1999) estimated an age for I Zw 18C not exceeding 0.2 Gyr.

We use here high signal-to-noise 4.5m MMT, 4m KPNO and Keck II spectroscopy to study the evolutionary status of I Zw 18C. We also discuss the nature of the extended emission in the outermost regions of I Zw 18. Our motivation for this study is the following. Until now, age estimates for the stellar populations in I Zw 18C are based solely on *HST* CMDs. While in principle CMD studies are powerful tools for studying stellar populations, they critically depend on the adopted distance to the galaxy and the interstellar extinction, which are a priori unknown. We use here distance-independent techniques based on spectroscopic observations to derive the age of the stellar populations in I Zw 18C.

Concerning the outermost regions of I Zw 18, while gaseous emission is an important contributor to the total light in the vicinity of the star-forming regions, there was no evidence for extended stellar emission at distances as far as $20''$ from the H II regions (e.g., Dufour et al. 1996b; Izotov et al. 1999). However, in some recent papers (e.g., Legrand 2000; Legrand et al. 2000; Kunth & Östlin 2000) such an old extended stellar population has been postulated. We use deep MMT and Keck II spectroscopic observations to clarify the origin of the extended emission and estimate the contribution of the ionized gas to it.

The observations and data reduction are described in Sect. 2. The properties of the stellar population in I Zw 18C are discussed in Sect. 3. In Sect. 4 we discuss the properties of the outlying regions of I Zw 18. Our results are summarized in Sect. 5.

2. Observations and data reduction

The Keck II spectroscopic observations of I Zw 18C were carried out on January 9, 2000 with the low-resolution imaging spectrograph (LRIS) (Oke et al. 1995), using the 300 groove mm^{-1} grating which provides a dispersion $2.52 \text{ \AA pixel}^{-1}$ and a spectral resolution of about 8 \AA in first order. The slit was $1'' \times 180''$, centered on the brightest central region (region C) of I Zw 18C and oriented with a position angle $\text{P.A.} = -80^\circ$ (slit orientation “1” in Fig. 1). No binning along the spatial axis has been done, yielding a spatial sampling of 0.2 pixel^{-1} . The total exposure time was 60 min, broken into three 20 min exposures. All exposures were taken at airmass of 1.42. The seeing was $0.9''$.

MMT spectroscopic observations of I Zw 18 and I Zw 18C were carried out in the nights of 1997 April 29 and 30. A signal-to-noise ratio $S/N \gtrsim 50$ was reached in the continuum of the bright

NW region of I Zw 18. Observations were made in the blue channel of the MMT spectrograph using a highly optimized Loral 3072×1024 CCD detector. A $1''.5 \times 180''$ slit was used along with a 300 mm^{-1} grating in first order and an L-38 second-order blocking filter. This yields a spatial resolution along the slit of $0''.3 \text{ pixel}^{-1}$, a scale perpendicular to the slit of $1.9 \text{ \AA pixel}^{-1}$, a spectral range $3600 - 7500 \text{ \AA}$, and a spectral resolution of $\sim 7 \text{ \AA}$ (FWHM). To improve the signal-to-noise ratio, CCD rows were binned by a factor of 2, yielding a final spatial sampling of $0''.6 \text{ pixel}^{-1}$. The total exposure time was 180 minutes broken up in six subexposures, 30 minutes each. All exposures were taken at airmasses $\lesssim 1.1 - 1.2$. The seeing during the observations was $0''.7$ FWHM. The slit was oriented in a position angle P.A. = -41° to permit observations of the NW and SE regions in I Zw 18 and the eastern region (region E) in I Zw 18C simultaneously (slit orientation “2” in Fig. 1).

The Kitt Peak 4m observations have been obtained on 18 March 1994 with the Ritchey-Chrétien RC2 spectrograph used in conjunction with the T2KB 2048×2048 CCD detector. We use a $2'' \times 300''$ slit with the KPC-10A grating ($316 \text{ lines mm}^{-1}$) in first order, with a GG 385 order separation filter. This filter cuts off all second-order contamination for wavelengths blueward of 7400 \AA which is the wavelength region of interest here. The above instrumental set-up gave a spatial scale along the slit of $0.69 \text{ arcsec pixel}^{-1}$, a scale perpendicular to the slit of $2.7 \text{ \AA pixel}^{-1}$, a spectral range of $3500 - 7500 \text{ \AA}$ and a spectral resolution of $\sim 5 \text{ \AA}$. All exposures were taken at airmass of 1.1. The seeing was $1''.5$. The slit was oriented along the SE – NW direction at a position angle of -41° , the same as that during the MMT observations (slit orientation “2” in Fig. 1). The total exposure time was 60 minutes and was broken up into 3 subexposures.

The spectrophotometric standard stars Feige 34 and HZ 44 were observed for flux calibration during each of three sets of the observations. Spectra of Hg-Ne-Ar (Keck II) and He-Ne-Ar (MMT and 4m KPNO) comparison lamps were obtained before and after each observation to provide the wavelength calibration.

Data reduction of spectral observations was carried out using the IRAF software package.⁴ This included bias subtraction, cosmic-ray removal and flat-field correction using exposures of a quartz incandescent lamp. After wavelength calibration, night-sky background subtraction, and correcting for atmospheric extinction, each frame was calibrated to absolute fluxes. One-dimensional spectra were extracted by summing, without weighting, different numbers of rows along the slit depending on the exact region of interest. We have extracted spectra of two regions in I Zw 18C (Fig. 1): (1) the brightest region C (Keck II observations) and (2) the eastern region E (all observations). The extracted spectra are shown in Fig. 2. Additionally, spectra of outlying regions of I Zw 18 at different distances from it have been extracted.

⁴IRAF: the Image Reduction and Analysis Facility is distributed by the National Optical Astronomy Observatory, which is operated by the Association of Universities for Research in Astronomy, Inc. (AURA) under cooperative agreement with the National Science Foundation (NSF).

3. The stellar population in I Zw 18C

One of the key problems discussed over the last three decades is the evolutionary status of I Zw 18: is this galaxy young or old? The evolutionary status of I Zw 18C has not been discussed in comparable detail. High signal-to-noise spectra of I Zw 18C reveal blue continua and show only emission and absorption hydrogen Balmer lines. Heavy element emission lines are not detected in the spectra, which precludes a metallicity determination of I Zw 18C. For the sake of simplicity we assume the heavy element mass fraction in I Zw 18C to be $Z_{\odot}/50$, the same value as in I Zw 18. However, the spectra obtained for I Zw 18C allow to study stellar populations and constrain their age with various techniques.

3.1. Age determination

A useful technique for determining the age of a galaxy is to fit its observed spectral energy distribution (SED) by theoretical SEDs calculated for various stellar population ages and star formation histories. This method (alone or in combination with photometric data) has been applied to some extremely metal-deficient BCDs with $Z = (1/20 - 1/40)Z_{\odot}$ (e.g., SBS 0335–052 (Izotov et al. 1997b; Papaderos et al. 1998), SBS 1415+437 (Thuan et al. 1999a), Tol 1214–277 (Fricke et al. 2001)). It was shown that, after subtraction of ionized gas emission, the underlying stellar components of these galaxies are consistent with populations not older than a few hundred Myr.

However, the spectral energy distribution fitting method is subject to uncertainties in the extinction, resulting in an age overestimate, if the adopted extinction is too low. Therefore, other methods are desirable to constrain the stellar population ages. We discuss in this Section two such methods, one relying on the Balmer nebular emission line equivalent widths and the other on the Balmer stellar absorption line equivalent widths.

3.1.1. Age from the nebular emission lines

On the assumption of a dust-free ionization-bounded H II region, the strongest hydrogen recombination emission lines $H\alpha$ and $H\beta$ provide an estimate of the age of the young stellar population when O and early B stars are still present. However, even if dust is present in H II regions, the age estimate is quite robust. This is because the ionizing flux from such a young stellar population and hence the equivalent widths of the Balmer emission lines have a very strong temporal evolution. Therefore, the dating method based on the $H\alpha$ and $H\beta$ emission lines is relatively insensitive to dust extinction.

The $H\alpha$ and $H\beta$ emission lines are detected in I Zw 18C in both regions C and E (Fig. 2). Their fluxes and equivalent widths are listed in Table 1. The exception is the Keck II spectrum of region E, where $H\beta$ emission was not detected. This non-detection is probably due to the patchy distribution

of the ionized gas. In Fig. 3a we compare the measured $H\alpha$ and $H\beta$ emission line equivalent widths with those predicted for an instantaneous burst as a function of age. The theoretical dependences have been kindly calculated for us by D. Schaerer using the Schaerer & Vacca (1998) code with the $Z = 0.0004$ Geneva evolutionary tracks from Lejeune & Schaerer (2001). They are shown by solid lines. The age derived from different hydrogen nebular emission lines in the various spectra is in a narrow range around ~ 15 Myr. Hence, the gas in I Zw 18C is likely to be ionized by early B stars.

3.1.2. Age from the hydrogen stellar absorption lines

Another method of stellar population age determination is based on the equivalent widths of absorption features. This method probes larger ages as compared to the previous method because the most prominent hydrogen absorption lines are formed in the longer-lived A stars.

Gonzalez Delgado & Leitherer (1999) and Gonzalez Delgado, Leitherer & Heckman (1999) have calculated a grid of synthetic profiles of stellar hydrogen Balmer absorption lines for effective temperatures and gravities, characteristics of galaxies with active star formation. They developed evolutionary stellar population synthesis models, synthesizing the profiles of the hydrogen Balmer absorption lines from $H\beta$ to $H13$ for an instantaneous burst with an age ranging from 10^6 to 10^9 yr. The calculations were made for a stellar initial mass function with Salpeter slope and with mass cutoffs $M_{\text{low}} = 1 M_{\odot}$ and $M_{\text{up}} = 80 M_{\odot}$.

The $H\gamma$, $H\delta$ and higher order hydrogen absorption lines due the underlying stellar populations are clearly seen in the Keck II spectra of I Zw 18C (Fig. 2a - 2b). Some hydrogen absorption lines are also seen in the 4m KPNO and MMT spectra (Fig. 2c - 2d). However, the signal-to-noise ratio is not high enough in the latter two spectra to measure equivalent widths. Although higher-order hydrogen Balmer absorption lines are seen in the spectrum of I Zw 18C, they are not suitable for age determination because of (a) the relatively low signal-to-noise ratio at short wavelengths and uncertainties in the placement of the continuum in the blue region caused by many blended absorption features, and (b) the weak dependence of their equivalent widths on age (Gonzalez Delgado et al. 1999).

In Table 2 we show the equivalent widths of the $H\delta$ and $H\gamma$ absorption lines measured in the spectra of regions C and E in I Zw 18C. We need to correct the equivalent widths of the absorption lines for the contamination by nebular emission. For region C we use the intensity of the $H\beta$ emission line to calculate the intensity of the $H\delta$ emission line adopting case B at the electron temperature of $\sim 20000\text{K}$ (e.g., Aller 1984). We do not use the $H\gamma$ absorption line in the spectrum of this region because of the strong contamination by nebular emission. The $H\beta$ emission line is not definitely detected in the Keck II spectrum of region E. For this region, the intensity of $H\alpha$ emission line is used to correct equivalent widths of the absorption lines for the same effect. The corrected equivalent widths of $H\delta$ and $H\gamma$ absorption lines are shown in Table 2.

In Fig. 3b we show by solid lines the predicted behaviour of the equivalent widths of the $H\gamma$

and $H\delta$ absorption lines with age for an instantaneous burst at a metallicity $Z = 1/20 Z_{\odot}$ (Gonzalez Delgado et al. 1999). The measured equivalent widths are shown for region C by filled circles and for region E by stars. Their values are consistent with an age of ~ 15 Myr. This age estimation is in excellent agreement with that obtained from the nebular emission line analysis implying that the light of I Zw 18C is dominated by a young stellar population. However, the age we derive here is significantly lower than the value of 40 Myr derived by Dufour et al. (1996b) for the brightest stars from *HST* CMDs of I Zw 18C.

3.1.3. Uncertainties

Although our two age estimates are consistent with each other, there are a number of uncertainties which may affect the result.

A major uncertainty is the unknown metallicity of the stars in I Zw 18C. We have assumed for simplicity the metallicity to be equal to that of the ionized gas in I Zw 18. Note, however, that a lower stellar metallicity would increase the age and vice versa.

To estimate an age from the emission lines we have assumed a dust-free ionization-bounded H II region. If the H II region is density-bounded or dust is present, then some of the ionizing photons escape the H II region or are absorbed. Equivalent widths of the Balmer emission lines give in this case an upper limit to the age.

Another source of uncertainty comes from the small number of massive stars in I Zw 18C. Our age estimates are based on models where the stellar initial mass function is well-behaved and can be approximated by an analytical function. However, small number statistics can introduce stochastic fluctuations at the high star mass end of the IMF. Recently Cerviño, Luridiana & Castander (2000) have analyzed how such stochastic effects influence the observed parameters of young stellar clusters with solar metallicity such as the $H\beta$ equivalent width and the number of the ionizing photons. The number of ionizing photons in I Zw 18C derived from the $H\beta$ emission line (Table 1) is $\sim 2 \times 10^{48} \text{ s}^{-1}$ and $4 \times 10^{48} \text{ s}^{-1}$ for the E and C regions respectively. With an equivalent width $\sim 6 - 7 \text{ \AA}$ of the $H\beta$ emission line, this corresponds to the case of a $10^3 M_{\odot}$ stellar cluster (Cerviño et al. 2000). For such a cluster the age variations at a fixed $H\beta$ equivalent width can be as high as 15 percent at the 90% confidence level. Hence, the age of I Zw 18C derived from the emission lines can lie in the range $\sim 10 - 25$ Myr, with a central value of 15 Myr. Similarly, age estimates based on absorption lines can also be slightly modified by stochastic effects. However, calculations are not yet available in the literature.

Gonzalez Delgado et al. (1999) do not calculate the temporal evolution of the equivalent widths of the Balmer absorption lines for the heavy element mass fraction $Z = Z_{\odot}/50$. Therefore, we use models with $Z = Z_{\odot}/20$. Extrapolation to the metallicity of I Zw 18 would result in a $\lesssim 1\text{\AA}$ decrease of the equivalent widths at a fixed age, or an age increase of up to 25 Myr.

Finally, the age determination depends on the star formation history in the galaxy which we consider next.

3.1.4. Continuous star formation

Our estimates for the stellar population age in I Zw 18C in Sect. 3.1.1 and 3.1.2 are based on the assumption of an instantaneous burst of star formation. Now we discuss how that age changes if continuous star formation is considered. We adopt a constant star formation rate in the interval between the initial time t_i when star formation starts and the final time t_f when it stops. Time is zero at the present epoch and increases into the past.

Using model equivalent width of the emission and absorption lines and spectral energy distributions for instantaneous bursts (Schaerer, private communication; Lejeune & Schaerer 2001; Gonzalez Delgado et al. 1999), we calculate the temporal evolution of the hydrogen emission and absorption line equivalent widths for continuous star formation. The results of calculations are presented in Figure 3. By dashed, dot-dashed and dotted lines are shown the temporal dependences of the equivalent widths of the $H\beta$ and $H\alpha$ emission lines (Fig. 3a), and of the $H\delta$ and $H\gamma$ absorption lines (Fig. 3b) for continuous star formation starting at time t_i , as defined by the abscissa value, and stopping at $t_f = 5, 8$ and 12.5 Myr, respectively. In other words, the equivalent widths of the above four lines in the spectrum of the stellar population formed between t_i and t_f have a value EW at time t_i in Fig. 3a and 3b. At a fixed EW , the general trend seen from Fig. 3 for continuous star formation is that the younger the youngest stars, the larger the time interval $t_i - t_f$, and the older the oldest stars. Another feature is that, at a fixed age t_f of the youngest stars, the age t_i of the oldest stars derived from the observed emission line equivalent widths, differs from that derived from the observed absorption line equivalent widths. In particular, in the model where star formation stopped 5 Myr ago (dashed lines), the age of the oldest stars derived from hydrogen emission lines exceeds 100 Myr, while the age of the oldest stars derived from hydrogen absorption lines is only ~ 50 Myr. This model seems to be excluded by consideration of the luminosity of the ionizing radiation. The most massive stars in the stellar population with age 5 Myr would have masses as high as $40 M_\odot$ (Meynet et al. 1994). The number of the ionizing photons produced by a single $40 M_\odot$ star is equal to $N(\text{Lyc}) \approx 1.5 \times 10^{49} \text{ s}^{-1}$ (Vacca, Garmany & Shull 1996), larger than that derived from the observed flux of the $H\beta$ emission line in I Zw 18C (Table 1), assuming an ionization-bounded H II region. There can be an upward correction factor of $\lesssim 2$ due to the extinction, but the corrected $N(\text{Lyc})$ would still be below the value for a single $40 M_\odot$ star. These estimates can however be modified by massive star small number statistics caused by the stochastic nature of star formation.

Though smaller, the difference between the age of the oldest stars derived from the equivalent widths of emission lines (50 Myr) and that derived from the equivalent widths of absorption lines (40 Myr), is present in the continuous star formation model with age of the youngest stars equal to 8 Myr (dot-dashed lines in Fig. 3). However, this difference is small in the continuous star

formation model which stopped 12.5 Myr ago (dotted lines). In this model, the age of the oldest stars should be ~ 25 Myr to consistently explain the observed hydrogen line equivalent widths.

Hence, similarly to the case of an instantaneous burst, we conclude that the observations of I Zw 18C are best reproduced by a short star formation episode which occurred continuously between ~ 10 Myr and ~ 25 Myr ago. Uncertainties in the observations and models may extend this range to between ~ 10 Myr and $\lesssim 100$ Myr ago.

3.2. Synthetic spectral energy distribution

A useful constraint on the stellar population age can be obtained from the spectral energy distribution. This method, as already noted, is subject to interstellar extinction. However, when used in conjunction with the methods discussed in Sect. 3.1 it provides a powerful tool for studying stellar populations by allowing to derive simultaneously the age and the extinction of the same region.

To fit the observed spectral energy distributions we use model SEDs calculated by D. Schaerer using the Schaerer & Vacca (1998) code and the $Z = 0.0004$ Geneva evolutionary tracks of Lejeune & Schaerer (2001). The contribution of the ionized gas was also included. This contribution is small because the equivalent widths of hydrogen emission lines in I Zw 18C are low.

Because the observed spectral energy distribution is extinction-dependent, the extinction can be obtained for regions with known ages as derived from the equivalent widths of the hydrogen emission and absorption lines. We consider the case of the 15 Myr instantaneous burst stellar population discussed in Sect. 3.1. First assume $C(\text{H}\beta) = 0$, where $C(\text{H}\beta) = E(B - V)/1.47$ (Aller 1984). Comparison of the observed Keck II spectra of regions C and E in I Zw 18C with the theoretical SEDs (bottom spectra in Fig. 4) shows that theoretical SEDs are bluer than the observed extinction-uncorrected spectra. Evidently, interstellar extinction is present in I Zw 18C and it modifies the observed SED. We derive $C(\text{H}\beta) = 0.3$ for region C and $C(\text{H}\beta) = 0.1$ for region E to achieve the best agreement between the extinction-corrected observed SEDs and the theoretical SEDs (upper spectra in Fig. 4). For comparison, we show in Fig. 4a by a dotted line the theoretical SED for a 40 Myr stellar population which does not provide as good a fit.

A theoretical 15 Myr stellar population SED also fits well the 4m KPNO and MMT spectra of region E extinction-corrected for $C(\text{H}\beta) = 0.1$ (Fig. 5). The theoretical 40 Myr stellar population SED with $C(\text{H}\beta) = 0.1$ fits less well (bottom solid line).

Some support for a larger extinction in region C than in region E comes from the observed $\text{H}\alpha$ -to- $\text{H}\beta$ flux ratios (Table 1). They are respectively equal to 4.5 and 3.8, corresponding to $C(\text{H}\beta) \sim 0.7$ and 0.4. However, correction for underlying stellar absorption results in lower extinction coefficients.

We note that we have not corrected the observed SEDs for the effect of atmospheric refraction.

If such an effect were to be important, it can selectively decrease the blue light relatively to the red light, leading us to derive erroneously high extinction for regions C and E. Indeed one may suspect that such an effect would be important for the Keck II spectrum which was obtained with a narrow slit of $1''$ at an airmass of 1.4. Filippenko (1982) has shown that atmospheric dispersion can produce an offset as high as $\sim 1''.2$ of the blue region near $[\text{O II}] \lambda 3727$ relative to the red region near $\text{H}\alpha \lambda 6563$ at this airmass. However, his calculations have been done for an altitude of 2 km, while the Keck II spectrum was obtained at an altitude about twice that. Furthermore, emission from the C component is extended and originates in a region significantly larger than the width of the slit, reducing the effect of the atmospheric dispersion. Perhaps the best argument for such an effect not to be important comes from the comparison of our different spectra of the same region. Although the Keck, MMT and 4m spectra of region E were obtained with different slit widths at different airmasses, they are all well fitted by the same 15 Myr single stellar population model.

We have thus reached two important conclusions for I Zw 18C: (1) the stellar population responsible for its observed SED is very young, with an age of ~ 15 Myr and (2) the region is characterized by a varying interstellar extinction implying the presence of non-uniformly distributed absorbing material. I Zw 18C is not the only very metal-deficient object to have a clumpy dust distribution. Earlier similar conclusions have been reached for the metal-deficient BCD SBS 0335–052 by Izotov et al. (1997b, 1999) and Thuan et al. (1997, 1999b). While the brightest and youngest star-forming region in SBS 0335–052 is relatively free of dust, extinction is higher at the location of the fainter and older super star clusters. Clumpy regions with large extinctions are clearly seen in the *HST* $V - I$ image of SBS 0335–052 (Thuan et al. 1997).

3.3. Photometric constraints

We have arrived at the conclusion that the light from I Zw 18C is dominated by stars ~ 15 Myr old. Is this conclusion consistent with the photometric data? In this section, we compare the predicted colors for the young stellar population with integrated broad-band colors of I Zw 18C obtained from ground-based and *HST* photometric observations. We also discuss the consistency between the properties of the stellar population in I Zw 18C obtained from the spectroscopic data with those obtained from analysis of *HST* WFPC2 CMDs.

3.3.1. Ground-based and *HST* broad-band photometry

In Table 3 we show the observed integrated V magnitude and colors of I Zw 18C. The second column shows these quantities without correction for interstellar extinction. Because the spectroscopic data imply the presence of extinction in I Zw 18C, we also show in the third column the colors corrected for interstellar extinction with $C(\text{H}\beta) = 0.3$ or $A_V = 0.65$ mag. These values are for the brightest region C. The extinction is lower in the fainter region E. The faint northwestern

region of I Zw 18C appears to be redder as compared to other regions (Dufour et al. 1996b), but the lack of spectroscopic data prevents us from determining the interstellar extinction in that region. We assume that the extinction derived for region C to be representative for the whole galaxy.

We compare the observed integrated colors of I Zw 18C with those predicted by instantaneous burst models for different ages. The first set of models shown in Table 3 is the same as the one used for fitting the SEDs with an heavy element mass fraction $Z = Z_{\odot}/50$ and based on Geneva stellar evolutionary tracks. Another set of predicted colors based on the Padua stellar evolution models has been calculated by Tantalo et al. (1996) for a single stellar population and a heavy element mass fraction of $Z_{\odot}/50$. Comparison of the two sets of models shows that colors based on the Padua stellar evolution models are systematically redder at a fixed age as compared to those based on the Geneva ones. Consequently, the use of Padua models results in younger ages as compared to Geneva models.

In the following we compare the observed colors to the modeled ones based on Geneva tracks. It is seen from Table 3 that the colors uncorrected for extinction are well reproduced by the model with a 100 Myr stellar population. However, with this age the predicted equivalent widths of the hydrogen emission lines are too small ($EW(H\beta) \lesssim 0.1\text{\AA}$, $EW(H\alpha) \lesssim 0.3\text{\AA}$) as compared to the observed ones (Fig. 3a). On the other hand, the predicted equivalent widths of the hydrogen absorption lines ($EW(H\delta) \gtrsim 10\text{\AA}$, $EW(H\gamma) \gtrsim 8\text{\AA}$) are too high (Fig. 3b). Again, to put observations into agreement with models, interstellar extinction has to be invoked. Indeed, all observed colors corrected for an extinction with $C(H\beta) = 0.3$ are in fair agreement with predicted ones for a 15 – 20 Myr single stellar population.

Our conclusions do not change significantly in the case of continuous star formation. In Fig. 6a – 6c we show by solid lines the theoretical dependences on age of the $(U - B)$, $(B - V)$ and $(V - I)$ colors in the case of constant continuous star formation, for different choices of t_i and t_f . The observed colors uncorrected for extinction (dashed lines) can be fitted by models with star formation starting at $t_i = 100 - 300$ Myr. However, these models predict too low an equivalent width for the $H\alpha$ emission line and too large an equivalent width for the $H\delta$ absorption line (Fig. 6d – 6e). Furthermore, models with star formation stopping at $t_f \gtrsim 40$ Myr are excluded for the whole range of t_i (Fig. 6d – 6e). To have the observed colors come into agreement with the observed equivalent widths of the Balmer lines, a non-negligible extinction must be assumed. We show by dotted lines in Fig. 6a – 6c the extinction-corrected colors with two values of the reddening, $E(B - V) = 0.1$ and 0.15 . In the latter case, the colors are explained by models with constant star formation starting at an age $t_i \sim 30 - 100$ Myr (filled and open circles) and stopping at an age $t_f = 8 - 12$ Myr. Observational uncertainties will only slightly increase this age range.

We conclude that our broad-band photometric data are consistent with a young stellar population and a non-negligible interstellar extinction in I Zw 18C. We emphasize that the ages derived above hold only for the brightest regions of the C component. We cannot exclude the possibility that the age of the stellar population in regions of I Zw 18C, not covered by our spectroscopic

observations, may be larger.

3.3.2. *Stellar color-magnitude diagrams*

CMD analysis is a powerful tool for studying stellar populations. However, as already pointed out, this method is sensitive to the adopted extinction and distance. While the extinction can be derived from spectroscopic observations, the determination of the distance is more uncertain.

A distance of ~ 10 Mpc to I Zw 18 has generally been adopted for analyzing the CMDs (Hunter & Thronson 1995, Dufour et al. 1996b and Aloisi et al. 1999). This assumes that the observed heliocentric radial velocity of the galaxy $\sim 740 \text{ km s}^{-1}$ is a pure Hubble flow velocity, and a Hubble constant $H_0 = 75 \text{ km s}^{-1} \text{ Mpc}^{-1}$. Adopting this distance would lead to a conflict with the well-observed ionization state of I Zw 18C. At 10 Mpc the brightest stars observed in I Zw 18C would have absolute V magnitudes fainter than -6 mag (Dufour et al. 1996b; Aloisi et al. 1999). In that case, comparison with evolutionary tracks implies that the most massive stars in I Zw 18C (called the C component by Dufour et al. (1996b)) would have masses less than $9 M_\odot$. The age of the stellar population with such an upper mass limit is at least 40 Myr (e.g., Dufour et al. 1996b), larger than the one derived from the equivalent widths of hydrogen emission and absorption lines ($\sim 10 - 25$ Myr). If the upper stellar mass limit of $9 M_\odot$ derived by Dufour et al. (1996b) and Aloisi et al. (1999) for I Zw 18C is correct, then ionized gas should not be present in it because of the absence of early B stars. But $H\alpha$ and $H\beta$ are clearly observed. Our derived age of ~ 15 Myr implies that early B stars with masses as high as $\sim 15 M_\odot$ are present in I Zw 18C, if an instantaneous burst of star formation is assumed. In the case of continuous star formation, the age of the youngest stars would be smaller and the upper mass limit larger to account for the presence of the ionized gas. We argue therefore that the stellar absolute magnitudes derived by Dufour et al. (1996b) and Aloisi et al. (1999) from their CMDs are too faint because they are based on too small an adopted distance. Östlin (2000) assumed a distance of 12.6 Mpc to analyze his *HST* NICMOS CMD. However, even this distance is not enough to explain the ionization state of I Zw 18C.

An additional effect is due to extinction, with $A_V = 0.65$ mag for the region C. Correcting for extinction and increasing the distance by a factor of ~ 1.5 to ~ 15 Mpc would make the most massive stars more luminous by a factor of ~ 4 and push the mass upper limit to $\sim 15 M_\odot$. A stellar population with such an upper mass limit would provide enough ionizing photons to account for the observed emission lines in I Zw 18C. Furthermore, the age of the brightest stars in the CMDs of I Zw 18C would be ~ 15 Myr, consistent with that derived from the hydrogen emission and absorption lines.

4. The extended emission in I Zw 18

Ground-based and *HST* $H\alpha$ and broad-band imaging have revealed filamentary structure around I Zw 18, inside a $15''$ radius (e.g., Hunter & Thronson 1995; Östlin, Bergvall & Rönnback 1996; Dufour et al. 1996b). Because of the presence of ionizing young stars, the light in these outlying regions is likely to be dominated by the emission of the ionized gas. This conclusion is supported by spectroscopic observations. Dufour et al. (1996a) and Izotov & Thuan (1998) have detected $H\alpha$ emission at distances as large as $20''$ from I Zw 18 in the NW direction of slit “2” (Fig. 1). Izotov et al. (1999) have found that at a distance of $\sim 5''$ to the northwest of the brightest NW region of I Zw 18, the equivalent width of the $H\beta$ emission line is $\sim 300\text{\AA}$. In this case the contribution of the gaseous continuum near $H\beta$ is ~ 30 percent of the total continuum. The contribution of the gaseous continuum near $H\alpha$ is even larger, being ~ 50 percent of the total continuum. Therefore, when analyzing stellar populations with the use of photometric data, it is essential to correct broad-band colors for ionized gas emission.

However, in some recent papers (e.g., Kunth & Östlin 2000) the extended emission around I Zw 18 has been attributed to an old stellar population, while the contribution of the ionized gas is assumed to be not dominant. That this cannot be true is seen in Fig. 7 where we show a map of the $H\alpha$ equivalent width distribution as obtained from *HST* narrow-band and broad-band images. While the $H\alpha$ equivalent width is small in the direction of the stellar clusters, it exceeds 1000\AA in the outer regions.

In the following, we analyze MMT and Keck II spectroscopic observations of the outer regions around I Zw 18 to clarify two issues: a) how important is the contribution of the ionized gas in the outer regions of I Zw 18? and b) is stellar emission present at large distances?

In Figure 8 we show the MMT spectrum of the region with a high $H\beta$ equivalent width. The spectrum is extracted within an aperture $1''.5 \times 3''$ (slit “2”), centered at a distance $5''$ to the northwest from the NW component of I Zw 18. It is characterized by strong emission lines. We refer to this region as the “ $H\alpha$ arc” (square box in Fig. 1). A synthetic spectrum with a 2 Myr stellar population combined with ionized gas emission fits best the observed SED of this region. The observed and extinction-corrected emission-line intensities in the $H\alpha$ arc together with their equivalent widths are listed in Table 4.

The ionic and elemental abundances have been derived following Izotov et al. (1994, 1997c). The extinction coefficient $C(H\beta)$ and the absorption equivalent width $EW(\text{abs})$ for the hydrogen lines are obtained by an iterative procedure. They are shown in Table 4 together with the observed flux $F(H\beta)$ of the $H\beta$ emission line. The electron temperature $T_e(\text{O III})$ was determined from the $[\text{O III}] \lambda 4363 / (\lambda 4959 + \lambda 5007)$ flux ratio and the electron number density $N_e(\text{S II})$ from the $[\text{S II}] \lambda 6717 / \lambda 6731$ flux ratio. The ionic and elemental abundances are shown in Table 5 together with ionization correction factors (ICFs). They are in good agreement with the abundances derived by Skillman & Kennicutt (1993), Izotov & Thuan (1998), Vílchez & Iglesias-Páramo (1998) and Izotov et al. (1999) for the NW and SE components of I Zw 18.

We have shown that the contribution of the ionized gas is large in the $H\alpha$ arc, at $\sim 5''$ from the NW component of I Zw 18. A similar situation prevails at significantly larger distances, as evidenced by deep Keck II spectroscopic observations. The slit during these observations (slit “1” in Fig. 1) crossed the outer regions of I Zw 18 including the expanding supershell of ionized gas best seen in $H\alpha$ images (e.g., Hunter & Thronson 1995; Dufour et al. 1996b). The latter feature located at $\sim 15''$ from I Zw 18 is labeled in Figure 1 as “LOOP”. We can thus study with deep spectroscopy the extended diffuse emission in I Zw 18 all the way from I Zw 18C to the bright star at the edge of Fig. 1 and located $\sim 40''$ from I Zw 18. In Fig. 9a – 9b we show respectively the flux distributions along the slit of the continuum near $H\beta$ and of the line + continuum emission at the wavelength of the $H\beta$ emission line. The origin is taken to be at region C. The locations of the bright star and loop are marked. In Fig. 9c we show the continuum-subtracted flux distribution of the $H\beta$ emission line. The negative values of the flux in some regions of I Zw 18C and around the star are probably caused by underlying stellar $H\beta$ absorption. No appreciable continuum emission is seen in Fig. 9a between I Zw 18C and the star. However, nebular emission of $H\alpha$ is present nearly everywhere between I Zw 18C and the star (Fig. 9c – 9d), suggesting that the contribution to the total flux of the nebular emission from ionized gas is important in the outermost regions, as far as $30''$ from I Zw 18.

In Fig. 9e we show the intensity distribution of the continuum at the wavelength of 4200\AA approximating the B band. We also plot by dotted lines the surface brightness levels in steps of $1 \text{ mag arcsec}^{-2}$. It is seen that the continuum surface brightness is fainter than $27 \text{ mag arcsec}^{-2}$ everywhere between I Zw 18C and the star, including the loop region. However, we cannot exclude the presence of stellar emission at the level of $28 \text{ mag arcsec}^{-2}$, as postulated by Legrand (2000). The contamination by extended ionized gas emission makes the detection of such an extremely faint hypothetical stellar background problematic.

In Fig. 10 we show the distributions along slit “2” of: a) the continuum intensity at 4200\AA , b) the continuum-subtracted flux and c) the equivalent width of the $H\alpha$ emission line. The distribution of $H\alpha$ emission (Fig. 10b) around the main body is more extended as compared to the continuum (Fig. 10a), the latter being confined in a region with radius less than $12''$ around the NW component. The equivalent width of $H\alpha$ is very high to the northwest of the NW component (Fig. 10c) and must be taken into account when photometric properties of the stellar population in I Zw 18 are analyzed. We also point out that the continuum distribution of region E in I Zw 18C is narrower than that of the $H\alpha$ emission line. The maximum $H\alpha$ equivalent width in region E (Fig. 10c) is offset to the northwest by $\sim 2''$ relative to the continuum distribution (Fig. 10a).

In Fig. 11 we show the spectrum of the loop. Despite its faintness, several emission lines are seen. However, the sensitivity in the blue region was not sufficient to detect the $[\text{O II}] \lambda 3727$ emission line. The continuum is very weak and can be significantly affected by uncertainties in the sky subtraction. This makes the measurements of line equivalent widths difficult. The fluxes and equivalent widths of the detected lines are given in Table 6. The flux errors include uncertainties in the placement of the continuum level and in the fitting of the lines by Gaussian profiles. However,

these errors do not take into account the uncertainties in the sky subtraction which might be large. Indeed, the loop flux in the continuum is only $\sim 1\%$ above the night sky flux, while that number is as high as 50% for the continuum flux in I Zw 18C. Even with these large uncertainties the emission line equivalent widths in the loop spectrum are very high. In particular, the equivalent width of the $H\beta$ emission line is 471 \AA or about half of the value expected for pure gaseous emission at the electron temperature $T_e = 20000\text{K}$. Hence, half of the flux in the continuum comes from the ionized gas, emphasizing again the importance of the correction of the spectral energy distribution and broad-band colors for gaseous emission. This goes contrary to the assumption of Kunth & Östlin (2000) that the contribution of gaseous emission does not affect the colors of the outlying regions of I Zw 18. If errors in the night sky subtraction are $\sim 1\%$, then the equivalent width of the $H\beta$ emission line in the loop spectrum is in the range $\sim 250 - 1000 \text{ \AA}$. Within the uncertainties, the emission of the loop is quite consistent with pure gaseous emission.

Kunth & Östlin (2000) have derived radial distributions of the surface brightness in the B band and of the $B - R$ and $B - J$ colors of I Zw 18 (their Fig. 8). They find that the colors rise continuously with increasing radius and reach $B - R = 0.6 \text{ mag}$ and $B - J = 1.6 \text{ mag}$ at a radius of $10''$. Assuming a purely stellar emission, they conclude that the observed colors can be reproduced by a single stellar population model with a metallicity of $1/50 Z_\odot$ and an age of $\log t = 9.1 \pm 0.1$ (t in yr), irrespective of the IMF (Bruzual & Charlot 2000, unpublished). However, this age estimate is rather uncertain and is dependent on the particular population synthesis model used. For example, Tantalo et al. (1996) using Padua stellar evolutionary tracks give values $B - R = 0.8 \text{ mag}$ and $B - J = 1.7 \text{ mag}$ for a 1 Gyr single stellar population with a metallicity of $1/50 Z_\odot$. The bluer colors derived by Kunth & Östlin (2000) would give an age of 100 – 300 Myr according to Tantalo et al. (1996)’ models. On the other hand, Leitherer et al. (1999)’ models using the Geneva stellar evolutionary tracks predict $B - R = 0.5 \text{ mag}$ and $B - J = 1.1 \text{ mag}$ for a 1 Gyr single stellar population with a metallicity of $1/20 Z_\odot$, bluer than those derived by Kunth & Östlin (2000). Leitherer et al. (1999)’ models do not go beyond 1 Gyr, but to reproduce the colors derived by Kunth & Östlin (2000), the age of the stellar population in the outer regions of I Zw 18, if present, must be older than 1 Gyr. Their models are calculated for a metallicity of $1/20 Z_\odot$, but colors with a metallicity of $1/50 Z_\odot$ are expected to be bluer, further increasing the derived age. These age estimates are very uncertain. The models by Leitherer et al. (1999) are less reliable for ages greater 100 Myr because they do not include asymptotic giant branch (AGB) star evolution. Tantalo et al. (1996) do include AGB star evolution, but the little known mass loss processes in the AGB phase introduce uncertainties in the predicted colors (Girardi & Bertelli 1998).

The next source of uncertainties comes from the photometric observations themselves. Beyond a radius of $\sim 5''$ from I Zw 18, the $B - R$ color profile derived by Kunth & Östlin (2000) increases monotonously while the $B - J$ color profile shows discontinuous jumps. These discontinuities are difficult to understand if the same stellar population is responsible for both colors. Kunth & Östlin (2000) do not show the uncertainties of their photometry. However, similar deep J -band photometry of another galaxy SBS 0335–052 (Vanzi et al. 2000) with UKIRT shows that at the

J -band surface brightness of $24 - 25$ mag arcsec $^{-2}$ the errors are already ~ 0.5 mag or more. New recent B and J photometric observations of I Zw 18 (Papaderos et al. 2001) do not confirm the large reddening of the $B - J$ color observed by Kunth & Östlin (2000) between radii $6''$ and $8''$, nor the discontinuous jumps.

To investigate whether the $B - R$ and $B - J$ colors of the extended emission can be explained by pure gaseous emission, we calculate the spectral energy distribution of the ionized gas emission in the corresponding wavelength range. The contribution of the free-bound, free-free and two-photon continuum emission is taken into account for the spectral range from 0 to $5 \mu\text{m}$ (Aller 1984; Ferland 1980). As for the electron temperature, we adopt the value of 19000K, which is the mean value between the electron temperatures in the NW and SE components of I Zw 18. Emission lines are superposed on the gaseous continuum SED with intensities derived from the observed spectrum of the loop at the distance of $\sim 15''$ from I Zw 18 (Table 6), in the spectral range $\lambda 3700 - 7500 \text{ \AA}$. Outside this range, the intensities of emission lines (mainly hydrogen lines) have been calculated from the extinction-corrected flux of $H\beta$ with reddening $A_V = 0.16$ mag. The reddening in the loop was calculated from the observed $H\alpha/H\beta$ flux ratio (Table 6), assuming an electron temperature $T_e = 20000\text{K}$. We derive $B - R = 0.8$ mag and $B - J = 0.9$ mag. If instead of the relative intensities of the emission lines observed in the loop, we use those seen in the NW or SE regions of I Zw 18 (Izotov et al. 1999), we obtain slightly bluer colors, $B - R = 0.6$ mag and $B - J = 0.7$ mag. The color difference is mainly due to a smaller contribution in the outer regions of some emission lines, e.g. $[\text{Ne III}] \lambda 3869$ to the B band. From this comparison we conclude that colors become redder at larger distances, even in the case of pure gaseous emission. While the $B - R$ color of gaseous emission is similar to the asymptotic value of ~ 0.7 mag derived by Kunth & Östlin (2000) at distances $\sim 15''$, the predicted $B - J$ color of gaseous emission is considerably bluer than the value they obtained. However, that value is consistent with $B - J \sim 0.6$ mag derived by Papaderos et al. (2001) in the $6 - 9$ arcsec radius range.

We note that the $B - R$ and $B - J$ colors are not ideal for constraining the existence of a possible extended low-surface-brightness 1 Gyr underlying stellar population in I Zw 18, the latter being uncertain, and the former being very similar to the color of ionized gas. The $B - I$ color is more useful because it can discriminate better between gaseous and a 1 Gyr stellar population emission. Indeed, adopting the relative line intensities in the $H\alpha$ arc or in the loop, the $B - I$ colors of the ionized gas emission are -0.1 mag and $+0.1$ mag respectively. The expected $B - I$ color for a 1 Gyr stellar population is much redder, $\sim +1.2$ mag (Tantalo et al. 1996). Observations give $B - I \sim 0$ at radii $8 - 10$ arcsec (Papaderos et al. 2001), strongly suggesting that the emission in the outer parts of I Zw 18 is gaseous in origin.

We conclude that there is no convincing observational evidence for the presence of an extended underlying low-surface-brightness stellar component in I Zw 18. Its existence, as postulated by Kunth & Östlin (2000), Legrand (2000) and Legrand et al. (2000), is neither supported by spectroscopic nor photometric observations.

5. Conclusions

We use spectroscopic and photometric data to constrain the age of the stellar population in the C component of I Zw 18 (\equiv I Zw 18C) and to study the origin of the extended emission around I Zw 18. We have arrived at the following main conclusions:

1. Deep 4m KPNO, MMT and Keck II spectra of I Zw 18C show $H\beta$ and $H\alpha$ hydrogen lines in emission, and $H\delta$ and $H\gamma$ hydrogen lines in absorption. Using their equivalent widths we derive an age of the stellar population of ~ 15 Myr if an instantaneous burst is assumed. If star formation is continuous, then the equivalent widths are best reproduced by a short star formation episode continuously occurring between ~ 10 Myr and ~ 25 Myr ago. Uncertainties in the observations and models may extend this range to between ~ 10 Myr and $\lesssim 100$ Myr ago.

2. Spectral energy distributions of the central (C) and eastern (E) regions of I Zw 18C are used to derive extinction. The equivalent widths of the hydrogen emission and absorption lines and the spectral energy distributions are modeled by a 15 Myr single stellar population if the extinction coefficient $C(H\beta) = 0.1 - 0.3$, corresponding to $A_V = 0.20 - 0.65$ mag.

3. With the usually assumed distance of ~ 10 Mpc the stellar population age derived from *HST* color-magnitude diagrams is too large as compared to the young age derived from the spectroscopic data. One possible source of the difference is interstellar extinction. Furthermore, to have agreement between the CMDs and the ionization state of I Zw 18C, the distance to the BCD should be increased to ~ 15 Mpc.

4. Concerning the extended emission around I Zw 18, Keck II spectra show $H\alpha$ emission as far as $30''$ from the main body. The equivalent widths of emission lines are particularly strong in the extended envelope ($EW(H\beta) = 471\text{\AA}$), implying a dominant contribution of the ionized gas emission in the outermost regions of I Zw 18. Within the large uncertainties of the continuum level, the emission at $\sim 15''$ from I Zw 18 is consistent with pure ionized gas emission. We do not find evidence for an old extended low-surface-brightness stellar component in the outlying regions of I Zw 18 down to the surface brightness level $B \sim 27$ mag arcsec $^{-2}$, contrary to suggestions by Kunth & Östlin (2000). It will be very difficult to detect the extended stellar emission at $B \sim 28$ mag arcsec $^{-2}$ postulated by Legrand (2000), because of the important ionized gas emission at large distances.

Y.I.I. and N.G.G. thank the Universitäts-Sternwarte of Göttingen for warm hospitality. We are grateful to D. Schaerer for making available his stellar evolutionary synthesis models in electronic form and for valuable comments on the manuscript. Y.I.I. thanks the Göttingen Academy of Sciences for a Gauss professorship. We acknowledge the financial support of the Volkswagen Foundation Grant No. I/72919 (Y.I.I., N.G.G., P.P. and K.J.F.), of DFG grant 436 UKR 17/1/00 (N.G.G.), Deutsche Agentur für Raumfahrtangelegenheiten (DARA) GmbH grants 50 OR 9407 6 and 50 OR 9907 7 (K.J.F. and P.P.), and of the National Science Foundation grants AST-9616863

(T.X.T. and Y.I.I.) and AST-9803072 (C.B.F.).

REFERENCES

- Aller, L. H. 1984, *Physics of Thermal Gaseous Nebulae*. Dordrecht: Reidel
- Aloisi, A., Tosi, M., & Greggio, L. 1999, *AJ*, 118, 302
- Cerviño, M., Luridiana, V., & Castander, F. J. 2000, *A&A*, 360, L5
- Davidson, K., Kinman, T. D., & Friedman, S. D. 1989, *AJ*, 97, 1591
- Dufour, R. J., Esteban, C., & Castañeda, H. O. 1996a, *ApJ*, 471, L87
- Dufour, R. J., Garnett, D. R., Skillman, E. D., & Shields, G. A. 1996b. In C. Leitherer, U. Fritze-v. Alvensleben, J. Huchra (eds.). *From Stars To Galaxies*. ASP Conference Series, vol. 98, p. 358
- Dufour, R. J., & Hester, J. J. 1990, *ApJ*, 350, 149
- Ferland, G. J. 1980, *PASP*, 92, 596
- Filippenko, A. V. 1982, *PASP*, 94, 715
- French, H. B. 1980, *ApJ*, 240, 41
- Fricke, K. J., Izotov, Y. I., Papaderos, P., Guseva, N. G., & Thuan, T.X. 2001, *AJ*, 121, 169
- Girardi, L., & Bertelli, G. 1998, *MNRAS*, 300, 533
- Gonzalez Delgado, R. M., & Leitherer, C. 1999, *ApJS*, 125, 479
- Gonzalez Delgado, R. M., Leitherer, C., & Heckman, T. M. 1999, *ApJS*, 125, 489
- Hunter, D. A., & Thronson, H. A., Jr. 1995, *ApJ*, 452, 238
- Izotov, Y. I., Chaffee, F. H., Foltz, C. B., Green, R. F., Guseva, N. G., & Thuan, T. X. 1999, *ApJ*, 527, 757
- Izotov, Y. I., Foltz, C. B., Green, R. F., Guseva, N. G., & Thuan, T. X. 1997a, *ApJ*, 487, L37
- Izotov, Y. I., Lipovetsky, V. A., Chaffee, F. H., Foltz, C. B., Guseva, N. G., & Kniazev, A. Y. 1997b, *ApJ*, 476, 698
- Izotov, Y. I., & Thuan, T. X. 1998, *ApJ*, 497, 227
- . 1999, *ApJ*, 511, 639
- Izotov, Y. I., Thuan, T. X., & Lipovetsky, V. A. 1994, *ApJ*, 435, 647
- . 1997c, *ApJS*, 108, 1
- Kinman, T. D., & Davidson, K. 1981, *ApJ*, 243, 147
- Kunth, D., & Östlin, G. 2000, *A&A Reviews*, 10, 1
- Legrand, F. 2000, *A&A*, 354, 504
- Legrand, F., Kunth, D., Roy, J.-R., Mas-Hesse, J. M., & Walsh, J. R. 1997, *A&A*, 326, L17
- . 2000, *A&A*, 355, 891

- Leitherer, C., Schaerer, D., Goldader, J. D., Gonzalez Delgado, R. M., Robert, C., Kune, D. F., de Mello, D. F., Devost, D., & Heckman, T. M. 1999, *ApJS*, 123, 3
- Lejeune, T., & Schaerer, D. 2001, *A&A*, 366, 538
- Lequeux, J., Peimbert, M., Rayo, J. F., Serrano, A., & Torres-Peimbert, S. 1979, *A&A*, 80, 155
- Martin, C. L. 1996, *ApJ*, 465, 680
- Meynet, G., Maeder, A., Schaller, G., Schaerer, D., & Charbonnel, C. 1994, *A&AS*, 103, 97
- Oke, J. B., Cohen, J. G., Carr, M., Cromer, J., Dingizian, A., Harris, F. H., Labrecque, S., Lucinio, R., Schall, W., Epps, H., & Miller, J. 1995, *PASP*, 107, 375
- Östlin, G. 2000, *ApJ*, 535, 99
- Östlin, G., Bergvall, N., & Rönneback, J. 1996. In D. Kunth, B. Guiderdoni, M. Heydari-Malayeri, T. X. Thuan (eds.). *The Interplay Between Massive Star Formation, the ISM and Galaxy Formation*. Gif-sur-Yvette: Edition Frontières, p. 605
- Pagel, B. E. J., Simonson, E. A., Terlevich, R. J., & Edmunds, M. G. 1992, *MNRAS*, 255, 325
- Papaderos, P., Izotov, Y. I., Fricke, K. J., Thuan, T. X., & Guseva N. G. 1998, *A&A*, 338, 43
- Papaderos, P., Izotov, Y. I., Noeske, K. G., Thuan, T. X., & Fricke, K. J. 2001, in *Dwarf Galaxies and their Environment*, eds: K.S. de Boer, R.-J. Dettmar, U. Klein, Shaker Verlag, in press
- Sargent, W. L. W., & Searle, L. 1970, *ApJ*, 162, 155
- Schaerer, D., & Vacca, W. D. 1998, *ApJ*, 497, 618
- Searle, L., & Sargent, W. L. W. 1972, *ApJ*, 173, 25
- Skillman, E. D., & Kennicutt, R. C., Jr. 1993, *ApJ*, 411, 655
- Tantalo, R., Chiosi, C., Bressan, A., & Fagotto, F. 1996, *A&A*, 311, 361
- Thuan, T. X., Izotov, Y. I., & Foltz, C. B. 1999a, *ApJ*, 525, 105
- Thuan, T. X., Izotov, Y. I., Lipovetsky, V. A. 1997, *ApJ*, 477, 661
- Thuan, T. X., Sauvage, M., & Madden, S. 1999b, *ApJ*, 516, 783
- Vacca, W. D., Garmany, C. D., & Shull, J. M. 1996, *ApJ*, 460, 914
- van Zee, L., Westpfahl, D., Haynes, M. P., & Salzer, J. J. 1998, *AJ*, 115, 1000
- Vanzi, L., Hunt, L. K., Thuan, T. X., & Izotov, Y. I. 2000, *A&A*, 363, 493
- Vílchez, J. M., & Iglesias-Páramo J. 1998, *ApJ*, 508, 248
- Zwicky, F. 1966, *ApJ*, 143, 192

Table 1. Parameters of emission lines in I Zw 18C

Line	Keck II				MMT		4m KPNO	
	region C		region E		region E		region E	
	F^a	EW^b	F^a	EW^b	F^a	EW^b	F^a	EW^b
H β	0.69 \pm 0.05	5.6 \pm 0.3	0.76 \pm 0.28	5.6 \pm 2.1	1.50 \pm 0.28	6.7 \pm 2.1
H α	3.08 \pm 0.06	49.7 \pm 1.0	0.61 \pm 0.03	21.1 \pm 1.1	2.78 \pm 0.26	51.8 \pm 4.9	5.72 \pm 0.26	62.5 \pm 4.9

^ain units of 10^{-16} erg s $^{-1}$ cm $^{-2}$.

^bin Å.

Table 2. Equivalent widths of absorption lines in I Zw 18C^a

Line	region C		region E	
	measured	corrected	measured	corrected
H δ	4.9 \pm 0.3	5.8 \pm 0.3	5.2 \pm 0.3	5.5 \pm 0.3
H γ	... ^b	...	4.0 \pm 0.3	4.7 \pm 0.3

^ain Å.

^bstrongly contaminated by emission.

Table 3. Integrated photometric properties of I Zw 18C

Param.	Observations ^a		Models						
			Geneva ^b				Padua ^c		
	$C(\text{H}\beta)=0$	$=0.3$	15Myr	20Myr	40Myr	100Myr	12.5Myr	15.8Myr	100Myr
(1)	(2)	(3)	(4)	(5)	(6)	(7)	(8)	(9)	(10)
V^{d}	19.20								
$U - B^{\text{e}}$	−0.50	−0.72	−0.83	−0.77	−0.59	−0.40	−0.81	−0.75	−0.37
$B - V^{\text{d}}$	0.00	−0.20	−0.17	−0.15	−0.08	−0.01	−0.18	−0.12	0.02
$V - I^{\text{e}}$	0.10	−0.17	−0.10	−0.08	0.04	0.13	−0.16	0.08	0.21
$V - K$	−0.15	−0.10	0.25	0.47	−0.25	0.29	0.67

^aMagnitudes and colors are corrected for interstellar extinction with the $C(\text{H}\beta)$ indicated.

^bBased on Geneva stellar evolutionary tracks with $Z=Z_{\odot}/50$ (Lejeune & Schaerer 2001).

^cBased on Padua stellar evolutionary tracks with $Z=Z_{\odot}/50$ (Tantalo et al. 1996).

^dDufour et al. (1996b).

^evan Zee et al. (1998).

Table 4. Emission line intensities in the H α arc

Ion	$F(\lambda)/F(\text{H}\beta)$	$I(\lambda)/I(\text{H}\beta)$	EW^a
3727 [O II]	0.361 \pm 0.038	0.374 \pm 0.040	53
3868 [Ne III]	0.139 \pm 0.040	0.143 \pm 0.042	20
3889 He I + H8	0.178 \pm 0.026	0.196 \pm 0.034	31
3968 [Ne III] + H7	0.212 \pm 0.026	0.230 \pm 0.034	39
4101 H δ	0.254 \pm 0.028	0.271 \pm 0.034	49
4340 H γ	0.455 \pm 0.036	0.470 \pm 0.041	106
4363 [O III]	0.040 \pm 0.016	0.040 \pm 0.016	13
4471 He I	0.034 \pm 0.014	0.034 \pm 0.014	9
4686 He II	0.019 \pm 0.011	0.019 \pm 0.011	7
4861 H β	1.000 \pm 0.060	1.000 \pm 0.061	292
4959 [O III]	0.460 \pm 0.036	0.454 \pm 0.036	179
5007 [O III]	1.417 \pm 0.079	1.399 \pm 0.079	551
5876 He I	0.069 \pm 0.014	0.067 \pm 0.014	40
6563 H α	2.902 \pm 0.140	2.755 \pm 0.146	1683
6678 He I	0.038 \pm 0.012	0.036 \pm 0.012	21
6717 [S II]	0.051 \pm 0.012	0.048 \pm 0.011	25
6731 [S II]	0.023 \pm 0.009	0.022 \pm 0.008	15
$C(\text{H}\beta)$	0.060 \pm 0.063		
$F(\text{H}\beta)^b$	0.12 \pm 0.01		
$EW(\text{abs}) \text{ \AA}$	2.3 \pm 3.2		

^ain \AA .

^bin units of $10^{-14} \text{ erg s}^{-1} \text{cm}^{-2}$.

Table 5. Heavy element abundances in the H α arc

Parameter	Value
$T_e(\text{O III})(\text{K})$	18200 ± 4000
$T_e(\text{O II})(\text{K})$	15100 ± 3200
$T_e(\text{S III})(\text{K})$	16800 ± 3400
$N_e(\text{S II})(\text{cm}^{-3})$	10 ± 10
$\text{O}^+/\text{H}^+(\times 10^5)$	0.316 ± 0.174
$\text{O}^{++}/\text{H}^+(\times 10^5)$	0.964 ± 0.504
$\text{O}^{+3}/\text{H}^+(\times 10^5)$	0.020 ± 0.016
$\text{O}/\text{H}(\times 10^5)$	1.301 ± 0.533
$12 + \log(\text{O}/\text{H})$	7.114 ± 0.178
$\text{Ne}^{++}/\text{H}^+(\times 10^5)$	0.206 ± 0.125
$\text{ICF}(\text{Ne})$	1.35
$\log(\text{Ne}/\text{O})$	-0.670 ± 0.365

Table 6. Parameters of the emission lines in the loop

Line	F^{a}	$F/F(\text{H}\beta)$	EW^{b}
3889 H ϵ +He I	0.73 ± 0.29	0.183	54
4101 H δ	0.91 ± 0.31	0.228	87
4340 H γ	1.56 ± 0.38	0.392	125
4861 H β	3.98 ± 0.96	1.000	471
4959 [O III]	0.59 ± 0.25	0.148	69
5007 [O III]	1.94 ± 0.42	0.487	229
6563 H α	11.55 ± 0.89	2.902	1396

^ain units of 10^{-16} erg s $^{-1}$ cm $^{-2}$.

^bin Å.

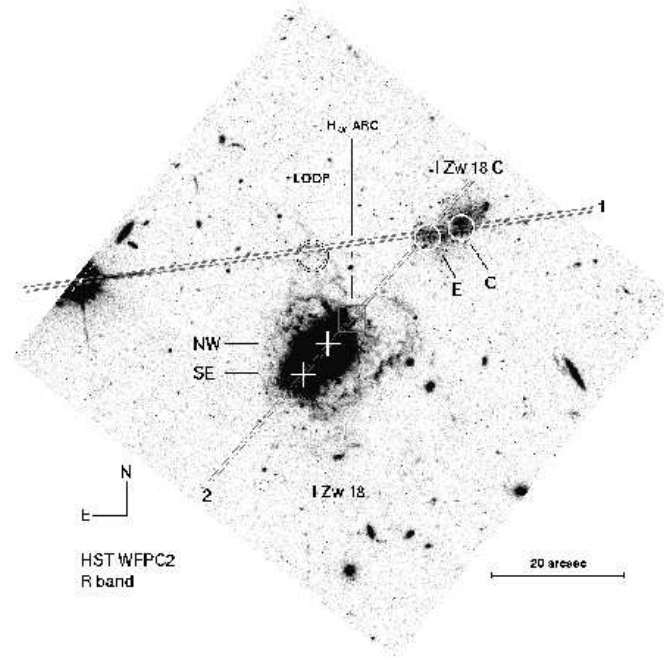


Fig. 1.— *HST* archival image of I Zw 18 in the *R* band. North is up, east to the left. The orientation of the slit during Keck II observations is shown as “1”, while the orientation of the slit during the 4m KPNO and MMT spectroscopic observations is shown as “2”. The two regions of star formation in I Zw 18 are marked as “SE” and “NW”. The locations of the outer regions with strong gaseous emission in I Zw 18 are labeled as “H α ARC” and “LOOP”. The locations of the central and eastern regions of I Zw 18C are labeled respectively as “C” and “E”.

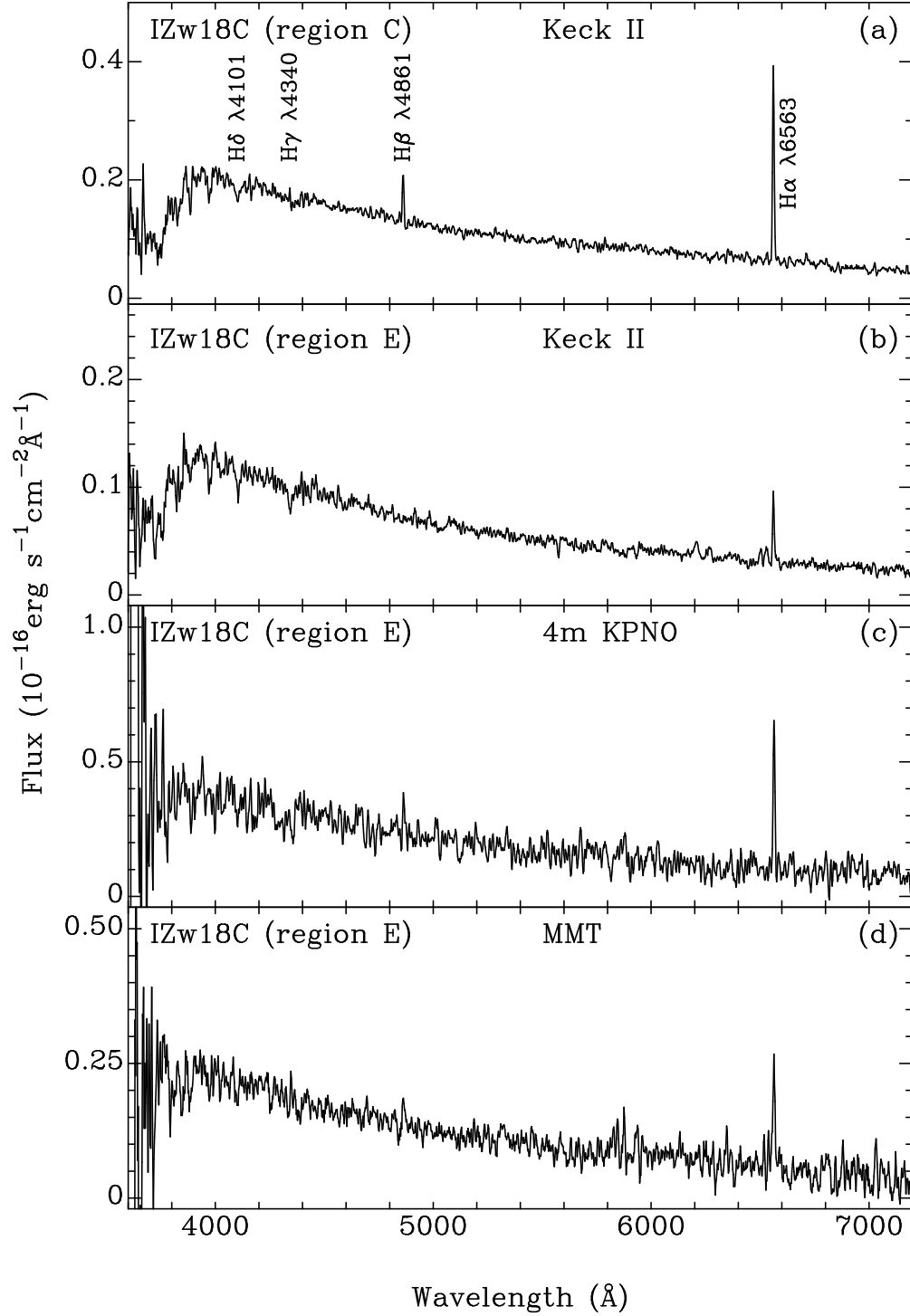


Fig. 2.— Keck II, 4m KPNO and MMT spectra of the central (C) and eastern (E) regions of I Zw 18C. Keck II spectra are extracted within a $0''.9 \times 1''$ aperture, the 4m KPNO and MMT spectra are extracted within $2'' \times 5''$ and $1''.5 \times 4''$ apertures respectively. The hydrogen emission and absorption lines are marked in the upper panel (a). All spectra are smoothed by a 3-point box-car.

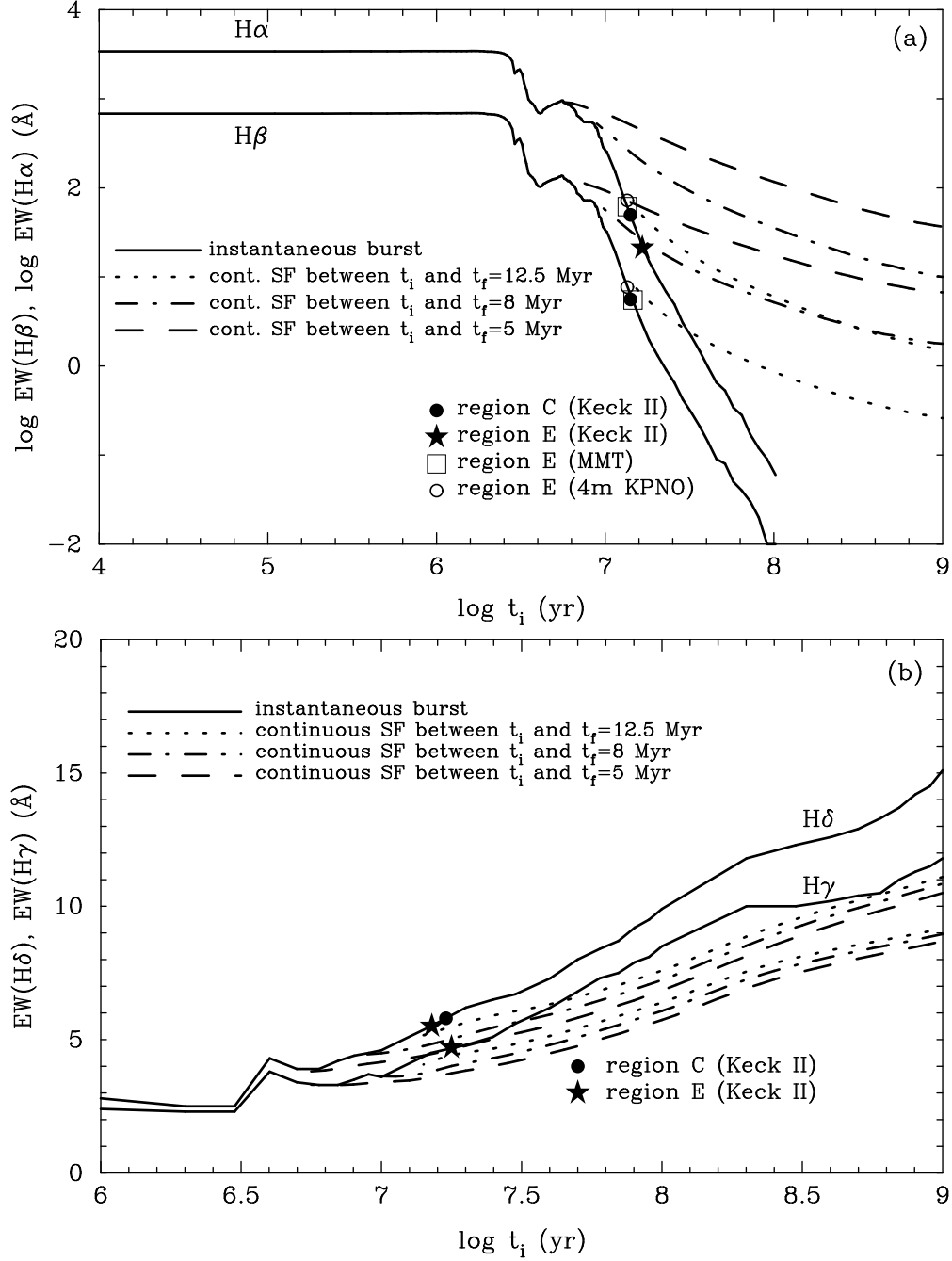


Fig. 3.— (a) Model dependences of the $\text{H}\alpha$ and $\text{H}\beta$ emission line equivalent widths on age for an instantaneous burst with the heavy element mass fraction $Z = Z_{\odot}/50$ (solid lines, Schaerer, private communication; Lejeune & Schaerer 2001). The measured $\text{H}\alpha$ and $\text{H}\beta$ equivalent widths are shown by different symbols and are consistent with a single stellar population age of $t = 15$ Myr. Model predictions are also shown for constant continuous star formation starting at an initial time defined by the abscissa t_i and stopping at a final time t_f , with $t_f = 5$ Myr (dashed line), $t_f = 8$ Myr (dot-dashed line) and $t_f = 12.5$ Myr (dotted line). Time $t_i = 0$ is now and increases to the past. (b) Model dependences of the $\text{H}\gamma$ (dashed line) and $\text{H}\delta$ (solid line) absorption line equivalent widths on age for an instantaneous burst with the heavy element mass fraction $Z = Z_{\odot}/20$ (Gonzalez Delgado et al 1999). The lines and symbols have the same meaning as in (a).

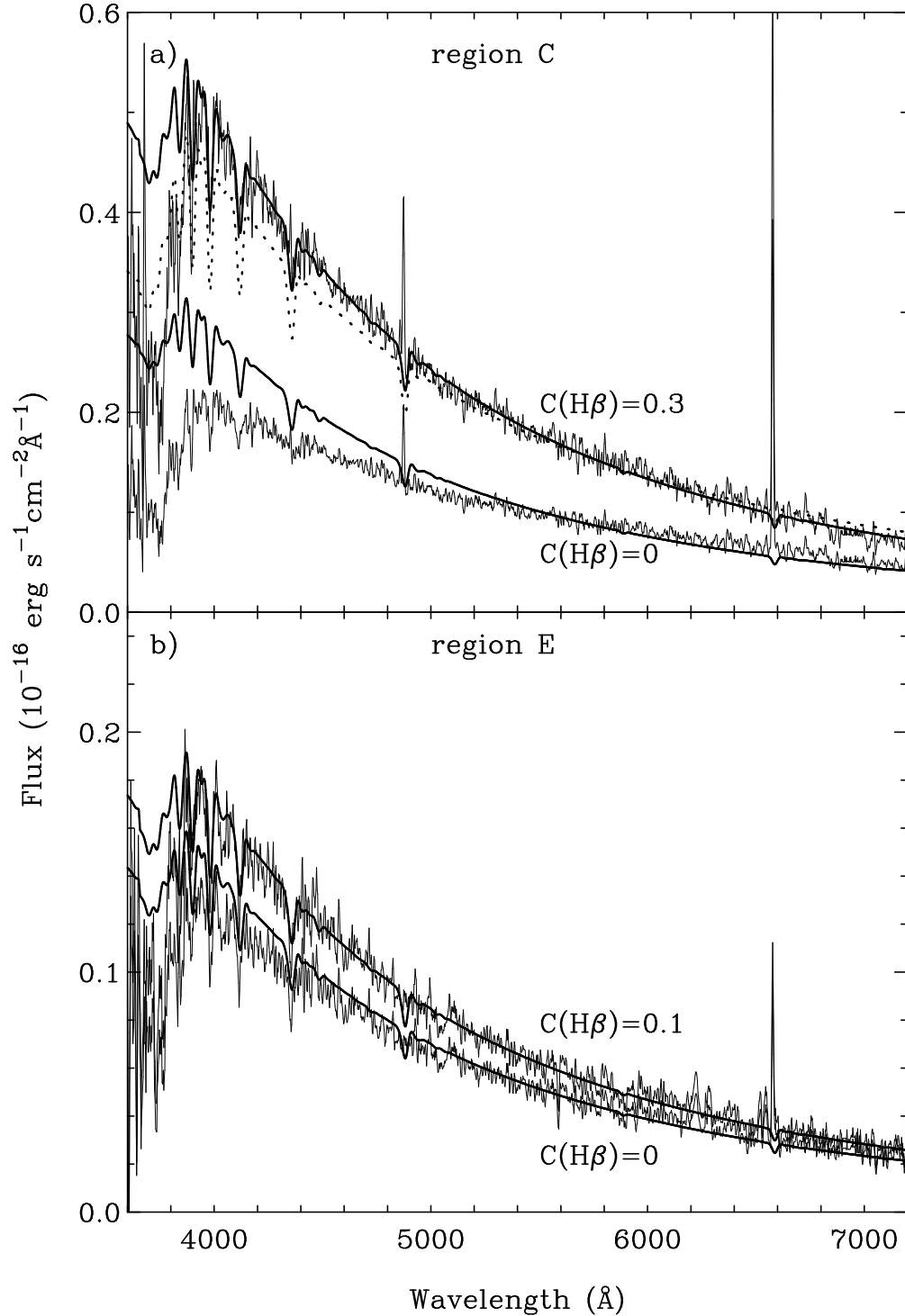


Fig. 4.— (a) Keck II spectra of region C in I Zw 18C corrected for reddening with two values of the extinction coefficient $C(\text{H}\beta) = 0$ and 0.3 (thin solid lines) on which are superposed model stellar population SEDs with age 15 Myr (thick solid lines). The dotted line is the model stellar population SED with age 40 Myr. (b) Keck II spectra of region E in I Zw 18C corrected for the reddening with two values of the extinction coefficient $C(\text{H}\beta) = 0$ and 0.1 (thin solid lines) on which are superposed model stellar population SEDs with age 15 Myr (thick solid line).

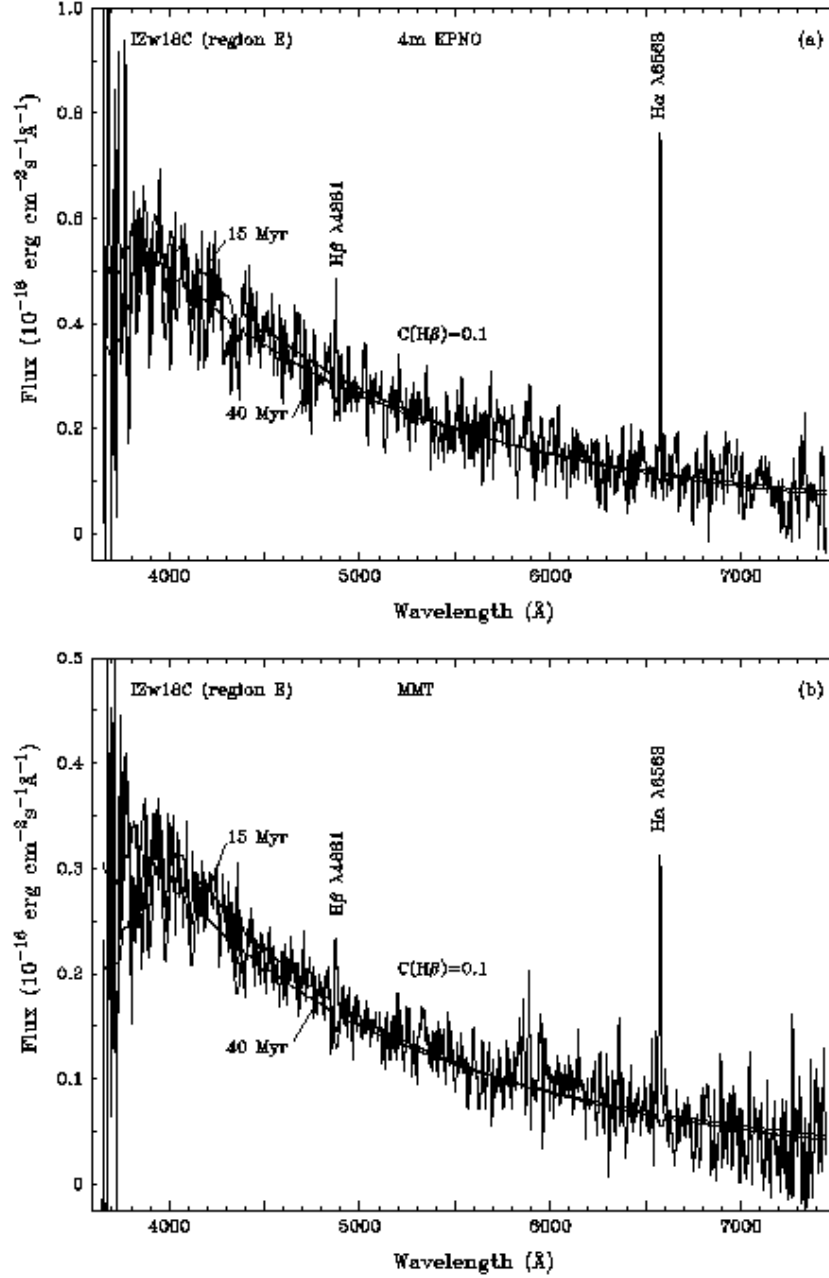


Fig. 5.— (a) 4m KPNO and (b) MMT spectra of region E in I Zw 18C (thin line) on which are superposed model stellar population SEDs with ages 15 Myr and 40 Myr (thick lines). The observed spectra are corrected for extinction with $C(\text{H}\beta) = 0.1$.

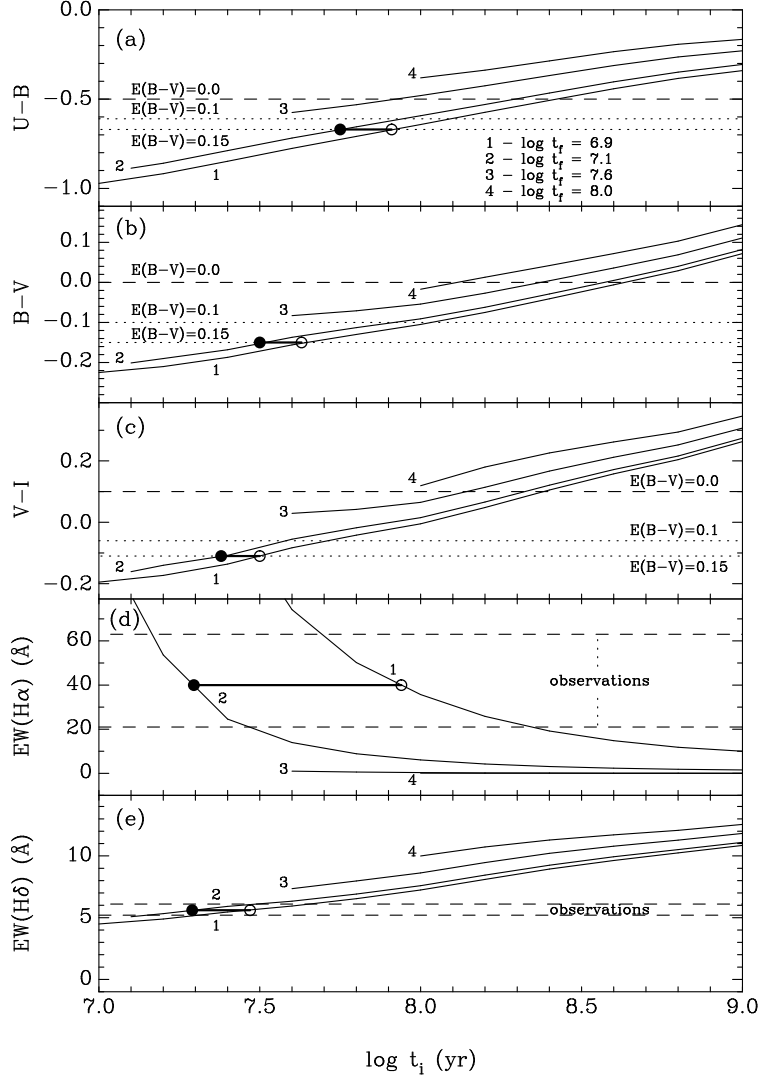


Fig. 6.— (a) - (c) Model dependences of the $(U - B)$, $(B - V)$, $(V - I)$ colors on age, for constant continuous star formation starting at an initial time defined by the abscissa t_i and stopping at a final time t_f , with a heavy element mass fraction $Z = Z_\odot/50$ (solid lines, Schaerer, private communication; Lejeune & Schaerer 2001). Curves with different t_f given in panel (a) are labeled from 1 to 4. The dashed lines show observed colors without correction for interstellar extinction. The dotted lines show colors corrected for interstellar extinction with $E(B - V) = 0.1$ and 0.15 . Open and filled circles mark the observed colors corrected for extinction with $E(B - V) = 0.15$ on the model lines with star formation stopping at $\log t_f = 6.9$ and 7.1 , where t_f is in yr. (d) - (e) Model dependences of the $H\alpha$ emission line ($Z = Z_\odot/50$, Schaerer, private communication; Lejeune & Schaerer 2001) and $H\delta$ absorption line ($Z = Z_\odot/20$, Gonzalez Delgado et al. 1999) equivalent widths on age, for constant continuous star formation starting at an initial time defined by the abscissa t_i and stopping at a final time t_f . The dashed lines show the range of observed equivalent widths. Open and filled circles show the location of the mean observed equivalent widths on the model lines for $\log t_f = 6.9$ and 7.1 .

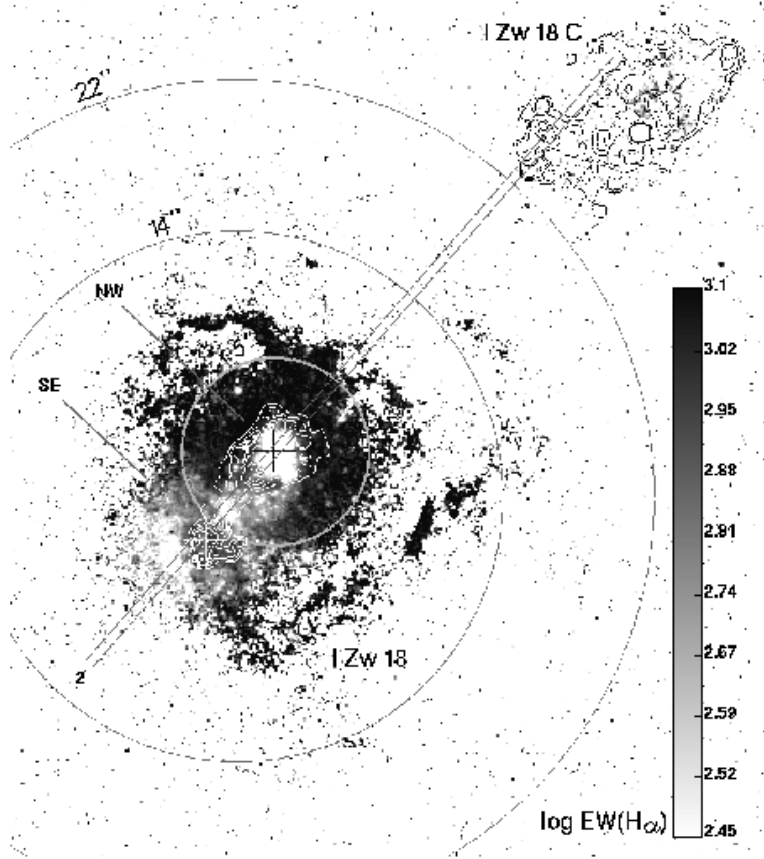


Fig. 7.— H α equivalent width map of I Zw 18 in the range between 280 Å and 1260 Å. The H α equivalent width increases from ~ 100 Å at the location of the NW star-forming region to ~ 1300 Å roughly 5" to the northeastern direction. This region, referred to as “H α arc” (see Fig. 1) coincides roughly with the intersection of the overlaid thick-grey circle with slit “2”. The larger circles with radii 14" and 22" are centered between the SE and NW regions.

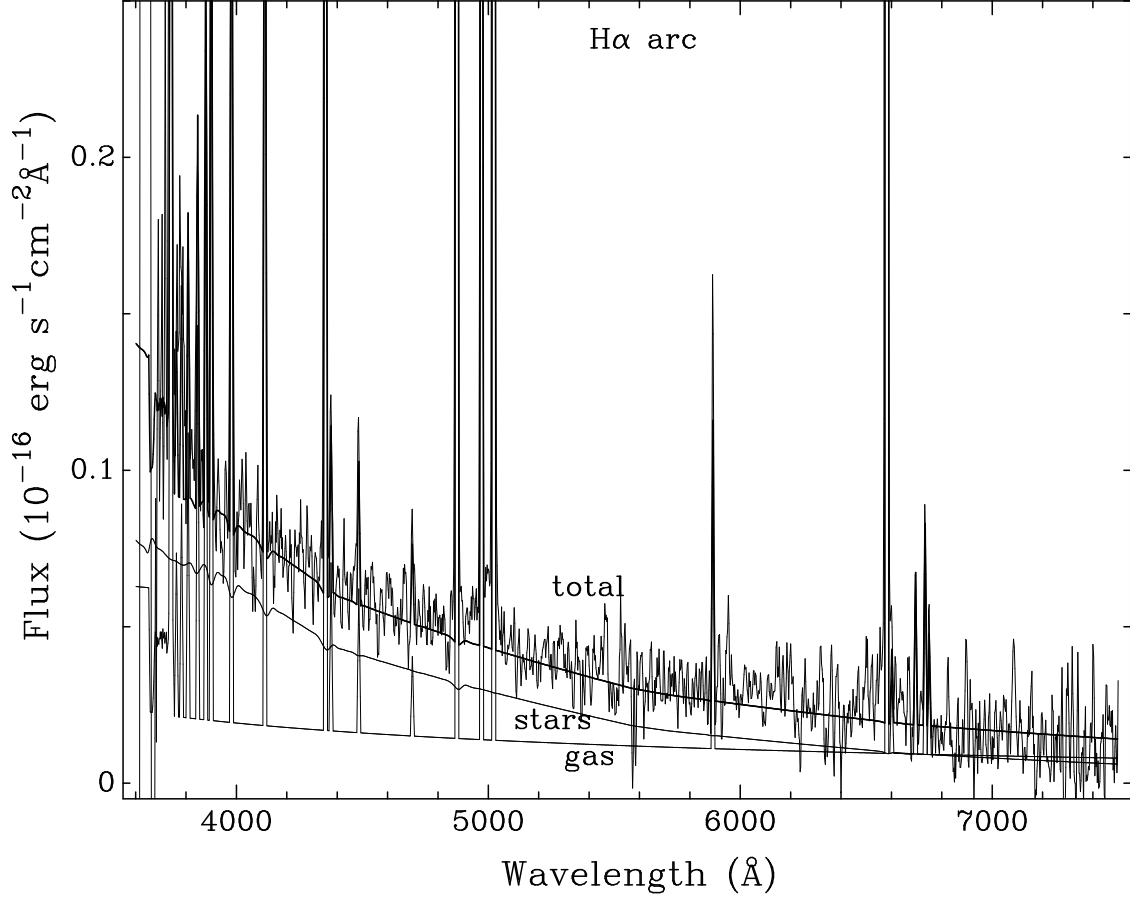


Fig. 8.— MMT spectrum of the H α arc in I Zw 18 (thin line) on which is superposed a synthetic continuum including both gaseous and stellar emission from a starburst with age 2 Myr (thick line). The spectrum is extracted within a $1''.5 \times 3''$ aperture, centered at a distance $5''$ to the northwest from the NW component of I Zw 18 (in slit “2”). It is corrected for an extinction $A_V = 0.13$ mag, derived from the Balmer hydrogen emission line decrement.

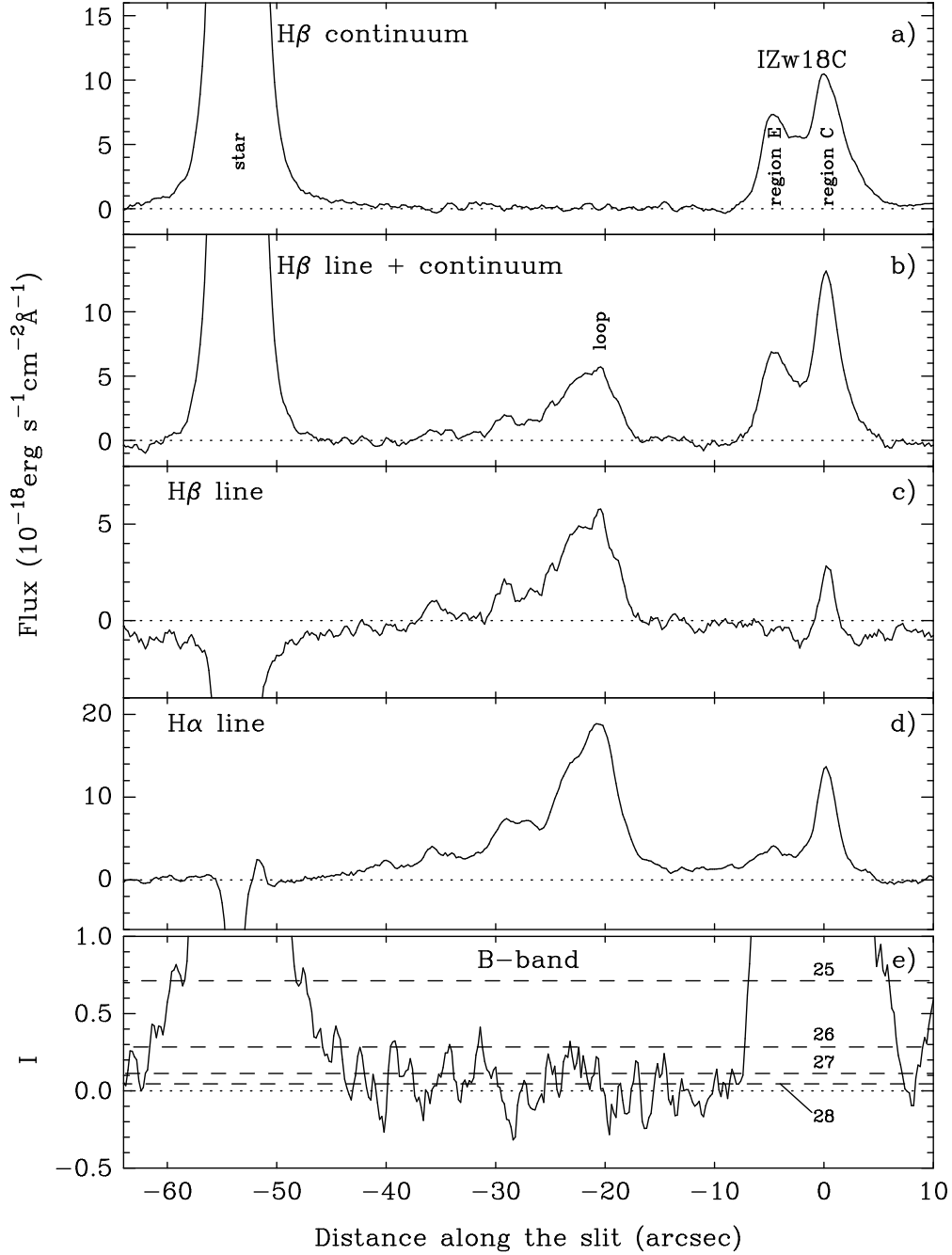


Fig. 9.— (a) Distribution of the $\text{H}\beta$ continuum flux along the slit from Keck II spectra with position angle -80° (slit “1” in Fig. 1). The locations of the E and C regions in I Zw 18C and the bright star (at the edge of Fig. 1) are marked. (b) The distribution of the $\text{H}\beta$ line + continuum flux along the slit. The location of the expanding shell is marked as “loop”. (c) Distribution of the continuum-subtracted $\text{H}\beta$ line intensity along the slit. (d) The distribution of the continuum-subtracted $\text{H}\alpha$ line flux along the slit. Note that $\text{H}\alpha$ emission is detected at a distance $\gtrsim 40''$ from region C of IZw18C, or at a distance as large as $\sim 30''$ from I Zw 18. (e) Distribution along the slit of the continuum intensity at $\lambda 4200$ in units $10^{-18} \text{ erg s}^{-1} \text{ cm}^{-2} \text{ \AA}^{-1} \text{ arcsec}^{-2}$. Different levels of the B surface brightness in mag arcsec^{-2} are shown by dashed lines.

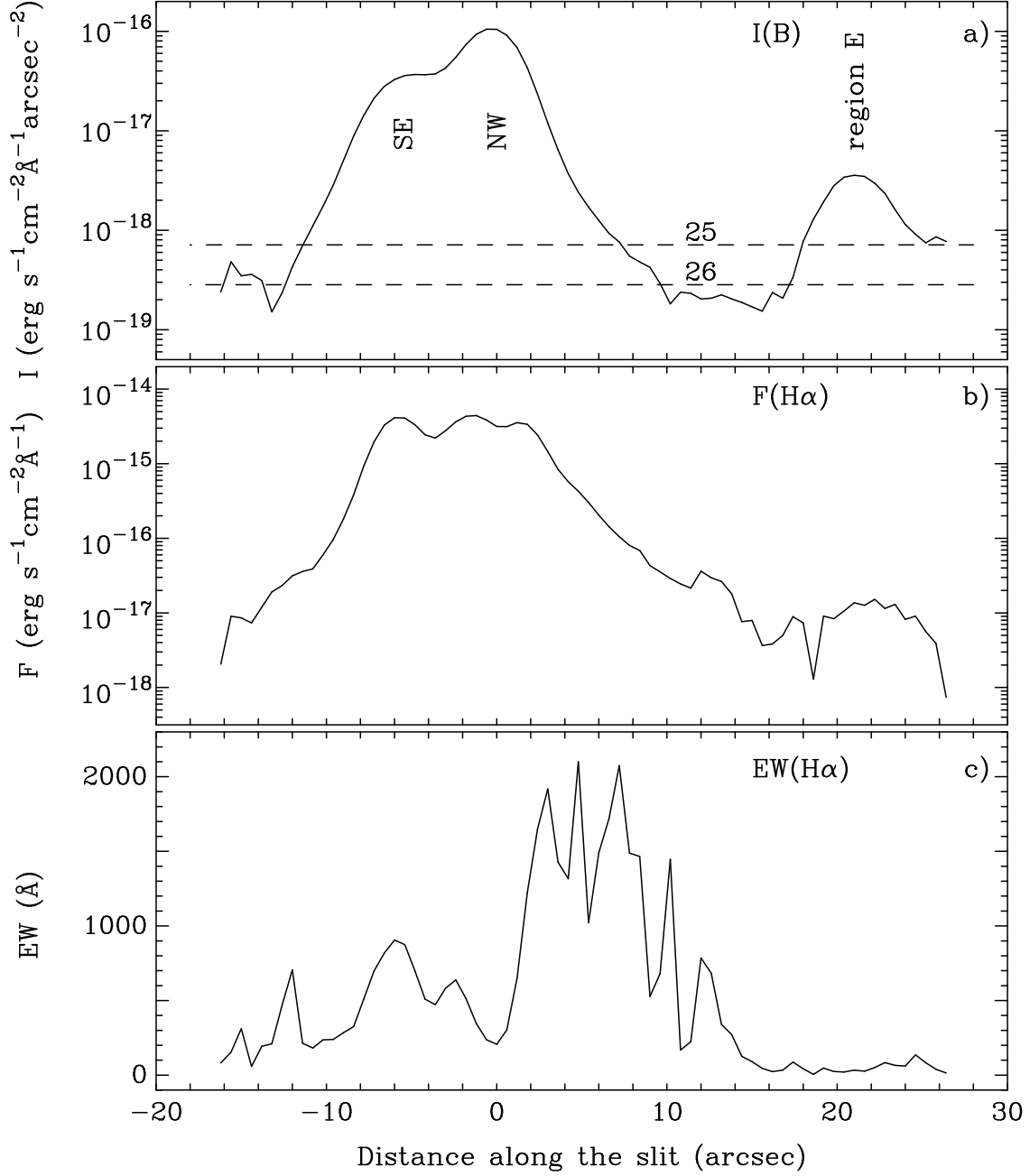


Fig. 10.— (a) Distribution of the continuum intensity at $\lambda 4200$ along the slit from MMT spectra with position angle -41° (slit “2” in Fig. 1). Different levels of the B surface brightness in mag arcsec^{-2} are shown by dashed lines. The distribution is smoothed by a 5-point box-car. The locations of the SE, NW components of I Zw 18 and region E of I Zw 18C are marked. (b) Distribution of the continuum-subtracted $H\alpha$ line flux along the slit. Note that the $H\alpha$ emission in the main body is more extended as compared to the continuum distribution. (c) Distribution of the $H\alpha$ equivalent width. Note the large values of $EW(H\alpha)$ to the northwest of the NW component implying an important contribution of gaseous emission to the total light in the extended region around the main body.

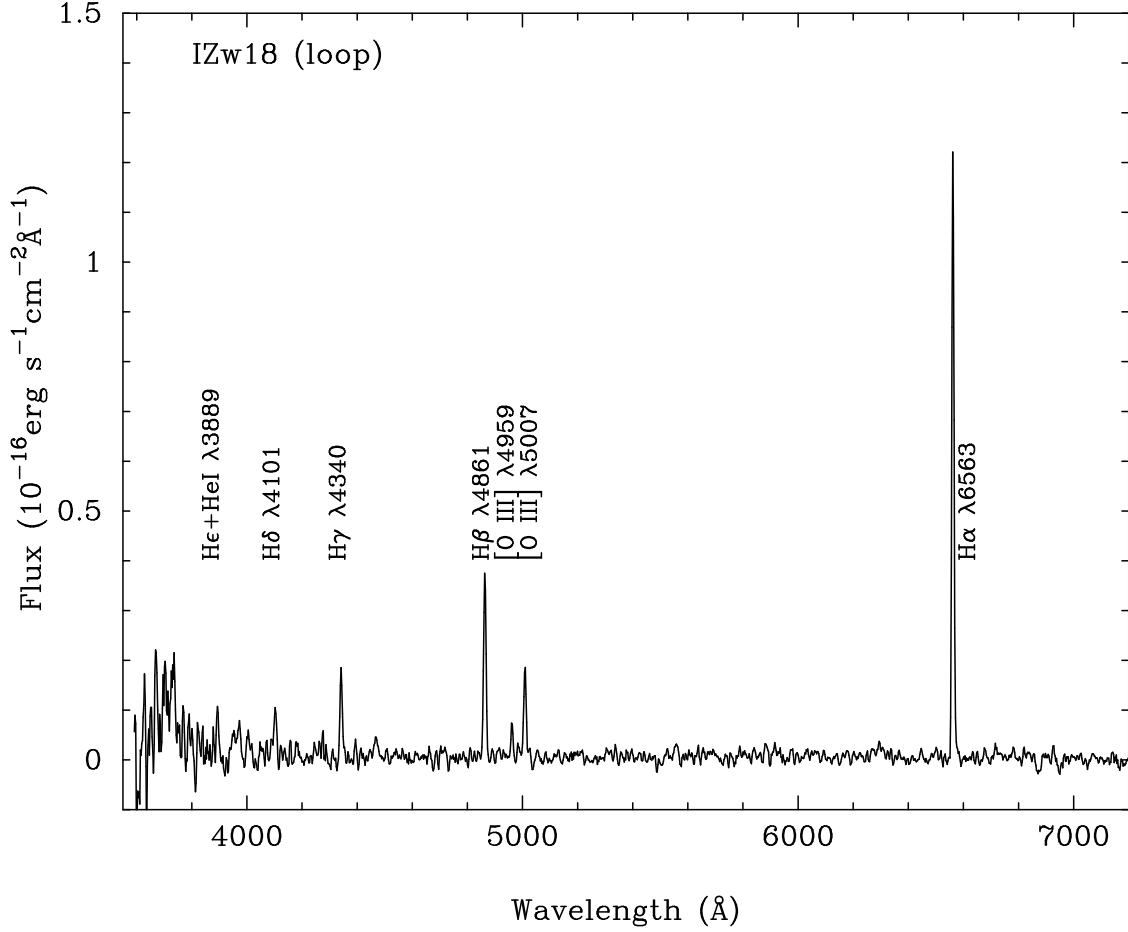


Fig. 11.— Spectrum of the expanding shell of I Zw 18 obtained with the Keck II (slit “1” in Fig. 1) and extracted in a $0''.9 \times 10''$ aperture at the distance of $\sim 15''$ from I Zw 18. The spectrum is smoothed by a 3-point box-car.